NASA CONTRACTOR REPORT

NASA CR-1583

EMITTANCE MEASUREMENT STUDY

by R. P. Heinisch, J. K. Andersson,
and R. N. Schmidt

Prepared by
HONEYWELL, INC.
Minneapolis, Minn.
for Langley Research Center

NATIONAL AERONAUTICS AND SPACE ADMINISTRATION • WASHINGTON, D. C. • MAY 1970

NASA CR-1583

EMITTANCE MEASUREMENT STUDY

By R. P. Heinisch, J. K. Andersson, and R. N. Schmidt

Prepared under Contract No. NAS 1-8447 by
HONEYWELL, INC.
Minneapolis, Minn.

for Langley Research Center

NATIONAL AERONAUTICS AND SPACE ADMINISTRATION

For sale by the Clearinghouse for Federal Scientific and Technical Information
Springfield, Virginia 22151 – CFSTI price $3.00

FOREWORD

This report documents the results of an Emittance Measurement Study performed for the National Aeronautics and Space Administration under Langley Research Center direction on contract No. NAS 1-8447. The study objective was to develop and implement an experiment to determine accurately the directional emittance of blackbody cavities. A comprehensive review of the literature was conducted on previous analytical and experimental studies, and results of those studies were incorporated. Four cavities were designed and tested during this study, and correlation of the test results with analytical prediction was made.

The cavities tested included straight conical, cylindrical, and two off-axis cones with entrance lips.

The Honeywell Aerospace and Systems and Research Divisions performed this study under the direction of Mr. J. C. Bates during the period 27 June 1968 through 18 May 1969.

Acknowledgment is extended to Mr. F. J. Bradac for fabricating the ellipsoidal reflector, to Dr. Hans Mocker who provided the laser, and to Mr. Douglas Perlick who programmed the analysis on the optical performance of the ellipsoid. The editorial assistance of Professor E. M. Sparrow of the University of Minnesota is gratefully acknowledged.

CONTENTS

ILLUSTRATIONS

ILLUSTRATIONS (Continued)

TABLES

SYMBOL LIST

E	radiant energy
ρ	reflectance
ϵ_λ	monochromatic emittance
α_λ	monochromatic absorptance
θ	angle of rays with respect to the normal to the cavity aperture
L/D	length-to-diameter ratio

EMITTANCE MEASUREMENT STUDY

By R. P. Heinisch, J. K. Andersson, and R. N. Schmidt
Honeywell Inc.

SUMMARY

A measurement technique was developed and tested for determining the directional spectral emittance of blackbody cavities. The emittance was determined from reflectance measurements of the cavities using a laser energy source (10.6 μ) and an integrating hemi-ellipsoid collector. It was demonstrated that this technique is capable of highly precise emittance measurements to a resolution of five significant figures for high emittance cavities.

Emittance measurements were made of four different blackbody cavities: a cylinder, cone, off-axis cone (all with length-to-diameter ratios of 3), and an off-axis cone (length-to-diameter ratio of 12:45). Measurements were made of each cavity coated with nominally specular and diffuse reflecting black paints. Additional measurements were made of the 12.45 length-to-diameter ratio off-axis conical cavity, without an internal paint coating.

Emittance values for these cavities varied from 0.94 for the cylinder painted with specular reflecting paint to greater than 0.99999 for the 12.45 length-to-diameter ratio, off-axis conical cavity when painted with either specular or diffuse reflecting paints.

INTRODUCTION

The concept of a blackbody is fundamental to the study and application of radiative transfer. A blackbody is defined as an ideal body that permits all incident radiation to enter and be absorbed internally. As a result, the blackbody is a perfect absorber, and therefore a perfect emitter if isothermal, which provides a standard against which real absorbers or emitters can be compared. In practice, it is difficult to obtain a good approximation to a blackbody due to a lack of experimental data on absolute emittance.

This investigation therefore was to determine precisely the directional spectral emittance of cavity radiators and to determine the specific performance of different cavity geometries. The technique employs Kirchhoff's law to calculate the spectral emittance based upon measurement of reflectance of a cavity. For the reflectance measurement, a monochromatic beam from a CO_2 laser is directed into the cavity aperture and radiation reflected out of the cavity in all directions is collected by an ellipsoidal mirror and brought to a focus on a detector. This experimental technique is capable of providing cavity emittance values of extremely high accuracy.

Emittance measurements at 10.6 μ were performed on four cavities during the investigation. The cavities of primary interest are two off-axis cones, the larger of which is geometrically equal to that being used at the NASA/Langley Research Center in an infrared calibration facility. In addition, emittance values were measured for a circular cylindrical cavity and a conical cavity. These configurations are commonly employed in engineering practice, and their performance was determined here as a basis for assessing the merits of the more sophisticated off-axis cavity designs. Experimental results for the cylindrical and conical cavities are amenable to a limited comparison with analytical predictions.

Tests were performed for various surface conditions within the interiors of the cavities. These included uncoated polished copper, a coating of black paint with approximately diffuse reflection characteristics, and a coating of black paint with approximately specular reflection characteristics.

LITERATURE SURVEY

An extensive survey of available literature pertaining to blackbody techniques and surface radiation properties was performed to complement the experimental investigation. This survey covered experimental studies, theoretical studies, and measurement techniques conducted previously.

The importance of the blackbody cavity concept, in the theory and application of radiative transfer, has been well documented. However, the survey showed that there have been very few experimental studies conducted to determine the quality of actual blackbodies used in experimental studies. Also, there is a definite lack of low-temperature work in the radiative transfer of energy from blackbody cavities.

Publications listed in the section "Bibliography" consist of 99 published works that were studied and applied to the design and conduct of this experiment. Major conclusions drawn from the survey are:

- Reliable measurements of spectral cavity emittance have not, heretofore, been performed.
- Analytical information on the spectral directional emittance of cavities is, to our knowledge, presently unavailable.
- Existing analytical predictions for the total hemispherical emittance of cavities are limited to elementary geometries. These have not been subjected to experimental verification.

THEORETICAL BASIS OF THE EXPERIMENTAL METHOD

The performance of blackbody cavities is generally defined in terms of fluxes of radiant energy which pass through the cavity aperture. Figure 1 schematically illustrates a blackbody cavity of arbitrary shape with incident and reflected energy. A parallel bundle of rays is directed into the cavity aperture, the rays being inclined at an angle of θ with respect to the normal to the cavity aperture. The incident radiant energy is denoted by E_i and the radiation reflected in all directions by E_r. Radiation properties of the cavity, i. e., emittance, reflectance, and absorptance, are defined as being equal to the radiation properties of the cavity aperture.

Reflectance of the cavity is given by:

$$\rho_\lambda(\theta) = \frac{E_r}{E_i} \tag{1}$$

where the subscript λ indicates monochromatic radiation properties. The absorptance is expressed as:

$$\alpha_\lambda(\theta) = \frac{E_i - E_r}{E_i} = 1 - \rho_\lambda(\theta) \tag{2}$$

By Kirchoff' s law, the monochromatic emittance ϵ_λ and monochromatic absorptance α_λ are equal for isothermal blackbodies. The equality is strictly valid for each angular direction (θ) and for each component of polarization. The present measurements are made with polarized radiation and therefore Kirchoff' s law is applicable without approximation.

Therefore,

$$\alpha_\lambda = \epsilon_\lambda = 1 - \rho_\lambda \tag{3}$$

where α is the directional absorptance, ϵ is the directional emittance and ρ is the hemispherical reflectance for directionally incident energy which indicates that directional emittance can be established if a technique is available for the measurement of hemispherical reflectance.

Using Equation (3), the sensitivity of the cavity emittance to errors in cavity reflectance is shown to be:

$$\Delta \epsilon_\lambda = \Delta \rho_\lambda = \rho_\lambda \frac{\Delta \rho_\lambda}{\rho_\lambda} \tag{4}$$

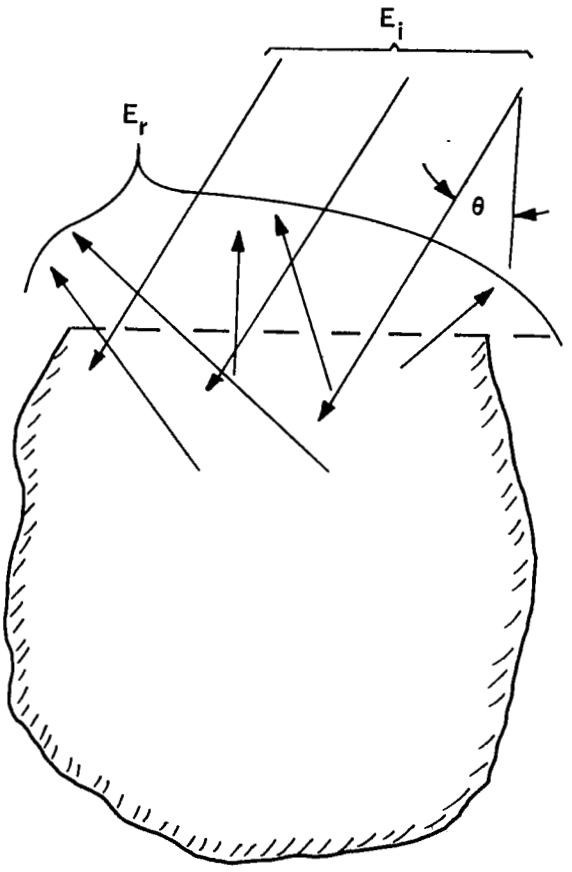

Figure 1. Arbitrary Blackbody Cavity Shape

To obtain precise values of the directional emittance ϵ_λ for bodies approximating a true blackbody cavity, large relative errors are permissable in measurement of reflectance ρ_λ. For a typical measurement of reflectance of 0.0005 with an error $\frac{\Delta\rho}{\rho}$ of 20 percent, the equivalent accuracy of the emittance calculation will be:

$$\epsilon = 0.9995 \pm 0.0001 \tag{5}$$

or 0.01 percent error.

REFLECTANCE EXPERIMENT

The experimental procedure used to obtain hemispherical reflectance measurements in the middle infrared to an accuracy much greater than previously attainable was made possible by the availability of a stable, highly-collimated, long-wavelength source, and the use of a specially constructed hemi-ellipsoidal mirror for collecting reflected energy and focusing it onto a detector.

Precision measurements of different cavities over long time periods required the use of such an energy source to ensure a continuous and precise level of input energy into the blackbody cavities. The ellipsoidal mirror used permitted positioning of the illuminated cavity at one focus and the detector at the second focus. This gave the detector an unobstructed view of the entire blackbody cavity since both focal points of the mirror were located side by side when viewed in the direction of the laser beam.

Previous hemispherical reflectance studies have used a hemispherical collector requiring that the blackbody cavity and detector be positioned off center. This resulted in an aperture image size distorted sufficiently to require integration of focused energy by movement of the detector. The integrating ellipsoidal collector permitted total reflected energy measurement using a large area detector fixed at the image focus.

Figure 2 schematically shows the measurement experiment. The modulated monochromatic beam from the laser enters the ellipsoidal collector and illuminates the blackbody cavity. Radiation which is reflected out of the cavity in all directions is collected by the ellipsoidal mirror and focused on a thermopile detector. Measurement accuracies using this reflectance experiment give cavity emittance values to five places.

The following sections of this report discuss in detail the cavities measured, the experiment design and error analyses, and the test results.

CAVITY CONFIGURATIONS

Selection of the blackbody cavities to be measured in this experiment was influenced by two primary factors. In the design and development of a precision long wavelength radiometer calibration source, an off-axis conical cavity with an entrance lip was used. Detailed analyses were made to define a cavity design that would approach unity emittance. Subsequent to the fabricating and testing of this system, however, no experimental verification of the absolute directional emittance was possible. Therefore, one of the cavities tested was dimensionally equal to the cavity designed for the radiometer calibration source (see (a) in Figure 3.)

Three additional cavities were tested to permit experimental and analytical data comparison and to compare data for off-axis conical cavities as a

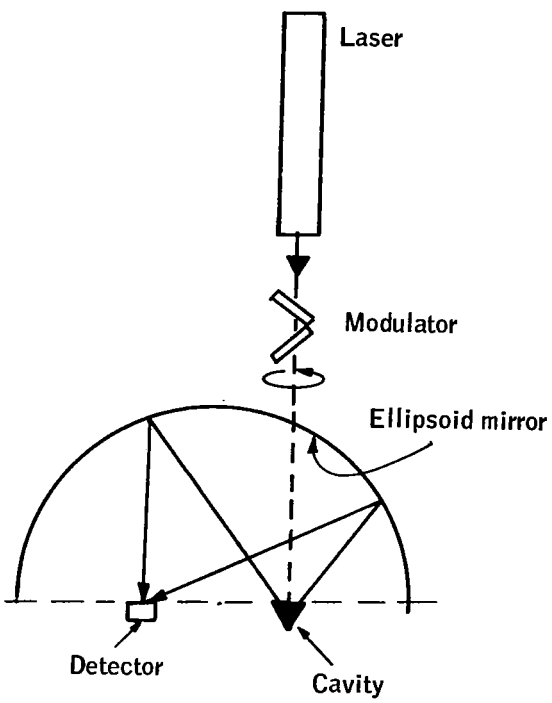

Figure 2. Laser Reflectometer

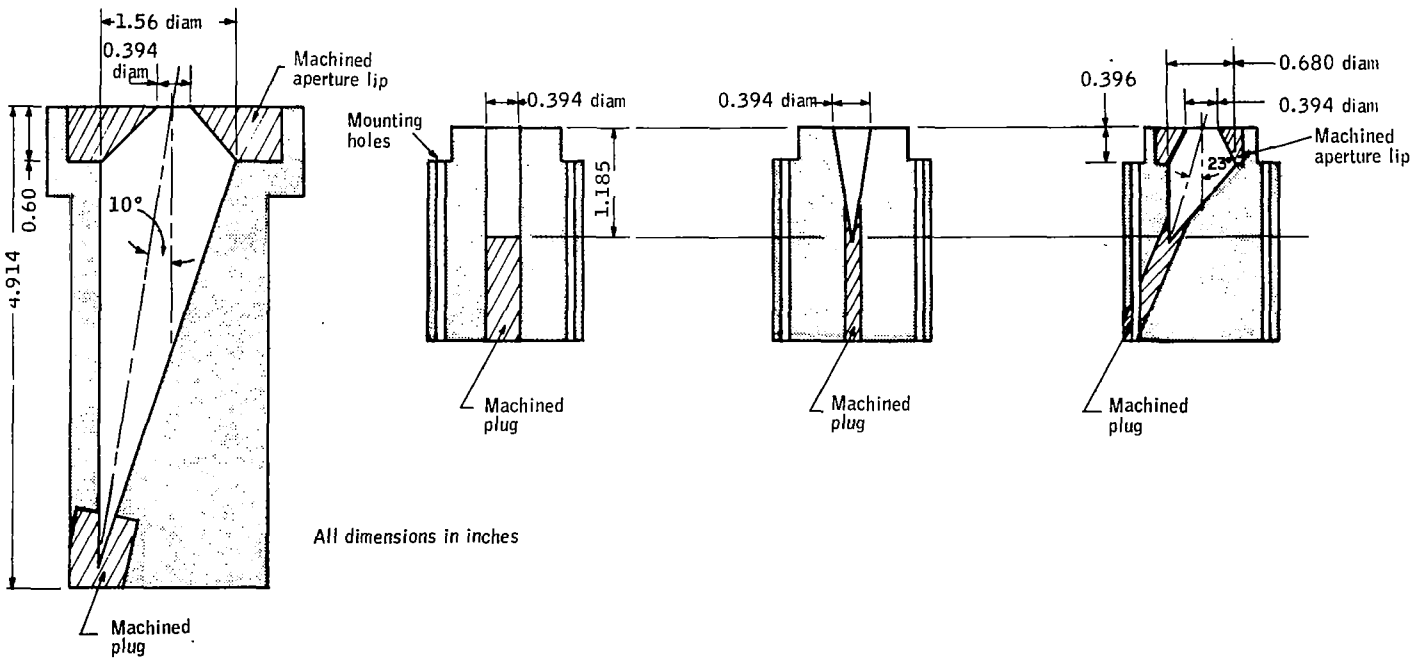

Figure 3. Blackbody Cavities

function of length to aperture diameter ratio. These cavity designs are presented in (b), (c), and (d) in Figure 3. The straight cylindrical and straight conical cavities represent simple geometric shapes that were amenable to a limited comparison with analytical data. A length-to-diameter ratio (L/D) of 3 provides cavity emissivities of approximately 0.99 to permit numerical comparison with the off-axis cone with a 12.45 L/D. This conical cavity was analytically designed to have an emissivity greater than 0.999.

All four cavities were fabricated from copper to reduce the possibility of significant thermal gradients along the cavity walls. Appendix A details the thermal analyses conducted and shows a maximum temperature cycle of 0.1°F at the laser energy input node.

Each of the cavities was tested using both nominally specular and nominally diffuse reflecting paints. In addition, the 12.45 L/D cavity was tested without any internal paint coating to permit determination of the effects of the paints. Reflectance measurements were made of paint samples on copper discs to determine if degradation of the paints occurred during laser illumination. These tests were made both before and after a 15-minute exposure to the incident laser beam and no significant changes to the paint surfaces were noted.

EXPERIMENT DESIGN

Integration of each of the individual elements of the experiment, error analyses conducted, and calibration of the equipment prior to actual measurements was accomplished with two primary goals: obtaining and maintaining experimental accuracy and facility of the measurements.

Mechanical design of the system test setup accomplished the necessary alignments, device motion requirements, and cavity insertion and extraction. Error analyses were conducted to determine both error sources and potential error magnitudes in the experimental data. Finally, two separate calibration methods were used, a calibration of the detector-electronics and a calibration of the entire system.

Each of the above elements of the experiment design is discussed in the following sections.

Apparatus

Figure 4 shows an isometric diagram of the experimental apparatus. The figure shows that radiation from the laser passes through, is chopped by the modulator, and enters through a slit opening in the ellipsoidal mirror into the blackbody cavity. The radiation is reflected from the cavity and is collected by the ellipsoidal collector and focussed onto the thermopile detector. The design provides for accurate positioning of the ellipsoid, detector, and cavities. The laser and modulator are mounted on a yoke which pivots about the major axis of the ellipsoid to permit varying the incidence angle of the laser beam on the cavity aperture.

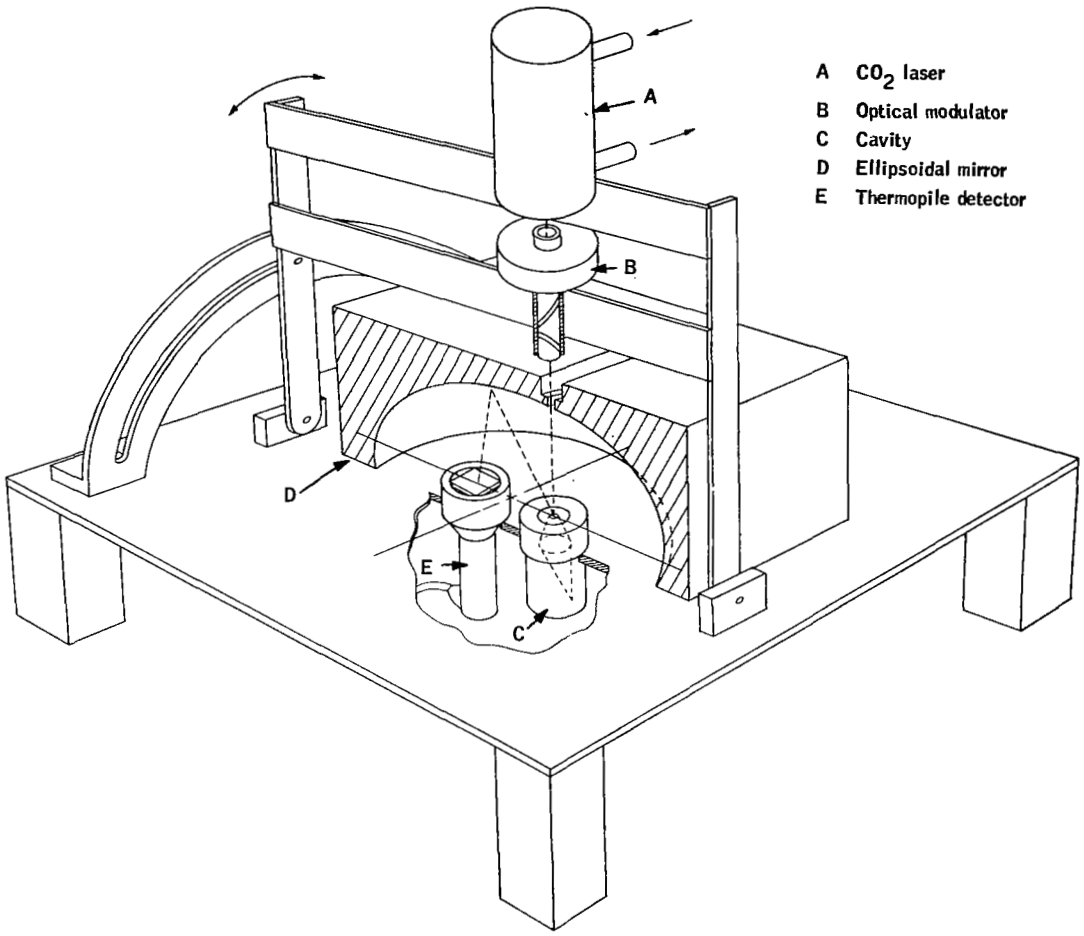

Figure 4. Isometric Diagram of Experimental Apparatus

To facilitate changing the blackbody cavities, provisions were made to permit insertion of the cavities from below while the ellipsoidal mirror remained in position. An additional rotational degree of freedom was provided to permit rotation to map directional emittance of the off-axis cavities.

Laser. -- The energy source used in the study is a sealed off single transverse mode (TEM_{ooq}), highly stable, single frequency CO_2 laser. The requirements for a long-term, stable energy source with very narrow beam characteristics dictated this choice. Long-term stability (one hour) of the laser output after a one-hour warm-up period was better than 0.1 percent.

Figure 5 shows the beam characteristics of the laser. These measurements were made at a distance of nine and a half feet from the laser where the beam spread has reached several inches. It is shown to be essentially free of diffraction effects, the secondary maxima occurring approximately four to five orders of magnitude below the center maximum.

To make reflectance measurements five orders of magnitude below the maximum beam intensity, background reflection off of the cavity entrance lip must be reduced to an equivalent level. Therefore, the laser was mounted in the test fixture to produce a beam diameter of 0.5 centimeter at the cavity aperture.

It was experimentally determined that less than 10^{-5} of the incident beam was reflected off the cavity aperture shoulder and imaged onto the detector. This was measured by replacing the blackbody cavities with a "dummy" cavity consisting of a hollow cylinder of similar shape. The primary beam passed through the hollow cylinder and was absorbed in the room housing the experiment. Only energy reflected off the aperture lip was collected and focused onto the detector (see Figure 6). With a highly polished aperture lip, the reflected energy was measured to be $< 10^{-5}$ of the incident beam and an order of magnitude lower with an absorbing surface on the entrance lip. Black flock paper was effectively used as the absorbing surface.

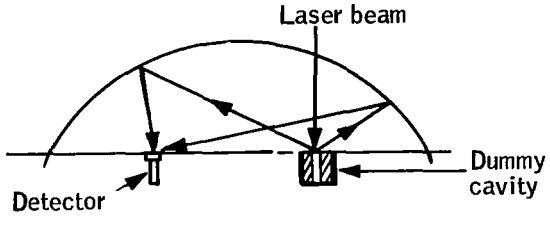

Figure 6. Calibration of Stray Reflection Off Cavity Shoulder

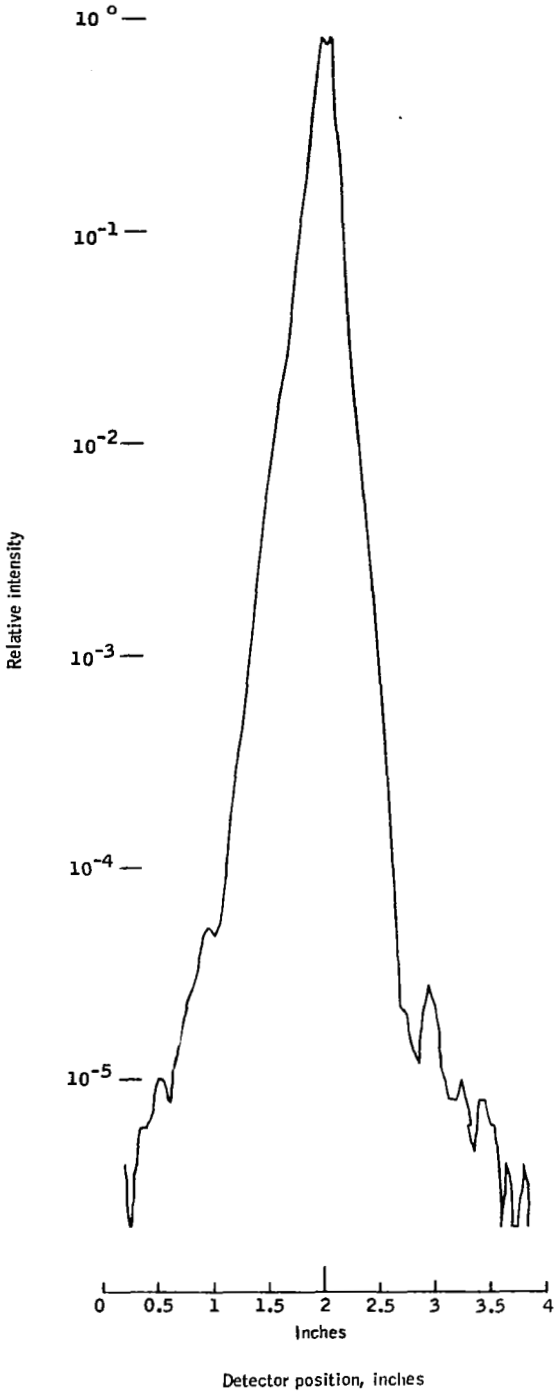

Figure 5. Laser Beam Characteristics at 9.5 Feet

Modulator. -- Modulation of the laser energy beam was required to distinguish the reflected input energy from the cavity and ellipsoidal collector self emissions. The chopping used an optical modulator to avoid the diffraction effects inherent in a mechanical chopper.

Figure 7 shows a schematic of the modulator assembly. The Irtran 2 optical flats are positioned within a hollow shaft which is rotated about the laser beam. Rotation of the shaft modulates the input energy by the change in reflection and transmission of the polarized laser beam. Two optical elements are used to null out lateral shifts of the beam so that the beam does not nutate about the laser axis with rotation of the modulator. Appendix B details the description and operational characteristics of the modulator.

A reference signal for the power lock-in amplifier was generated with a chopper blade attached to the modulator barrel. A small tungsten source and a photodiode were used for the lock-in signal generation at a 17-Hz chopping frequency.

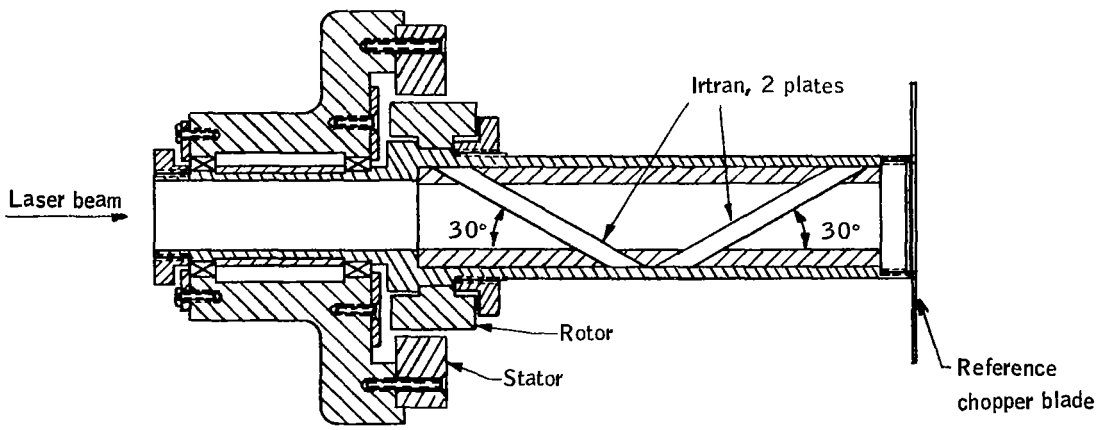

Figure 7. Modulator

Ellipsoidal mirror. -- An ellipsoidal mirror was constructed and used to collect the reflected energy fromthe cavities and focus it on the detector. An integrating hemisphere, commonly used for this purpose, was analyzed and found to be undesirable due to poor image quality resulting in increased measurement complexity and loss of accuracy. Figure 8 illustrates the improvement in image quality with use of an integrating ellipsoidal mirror rather than a hemispherical mirror. The diameter of the hemisphere and the major axis of the ellipsoid used for this analysis was 20 cm.

The ellipsoidal mirror constructed had semi-major and semi-minor axes of 5.0 and 4.8 inches, respectively, with a displacement focus from the center of 1.4 inches. The mirror surface is evaporated aluminum on an epoxy molded surface backed up with an aluminum coating for support and mounting. Appendix C details the design, construction, and tests of the ellipsoidal mirror.

Extensive theoretical analyses and experimental testing determined the optical performance of the ellipsoidal mirror. A computer program studied the imaging quality of the mirror of a 1-cm source aperture at one focus using a ray trace technique. Figure 9 shows the analytically determined image produced on a cathode ray tube display for 25 000 random ray traces from a diffuse source. Very little distortion is evident in the image of the 1-cm diameter source.

Experimental image quality measurements were made using visible light. Figure 10 shows a photograph of a 1-cm diameter diffuse light source and an image of that source generated by the ellipsoidal mirror. Approximately the same image distortion is evident as that predicted by the theoretical studies.

To obtain quantitative data on the reflectance of the ellipsoidal mirror surface at 10.6 μ, small flat samples of the mirror surface material were prepared in the same manner as the ellipsoid. Measurement of these surfaces with a reflectometer showed reflectances of the samples that varied from 0.87 for poor quality substrate to 0.94 for a good quality substrate. The ellipsoidal mirror surface was, except for a few extremely small spots, of good optical quality. For correction of the measurement data for mirror reflectance, a reflectance value of 0.93 was used. The significance of using this reflectance data to correct the test data is presented later in the error analysis discussions.

Detector. -- An evacuated thermopile detector was selected for use on this experiment. Many detectors were considered but the need for a large area detector with a wide field of view resulted in the selection of a specially prepared thermopile. The detector had a 3/4-inch square sensitive area covered with an Irtran 2 window. Responsivity of the detector was 2 microvolts per microwatt with a time constant of 5 milliseconds. Detector resistance was about 25 ohms with a noise equivalent power of 10^{-9} watt.

Angular and spatial sensitivities of the detector were measured with laser beams having beam diameters of 0.093 and 0.25 inch. The two size beams were used to ascertain narrow and wide beam response of the detector spatially across the detector sensitive element. Measurements were made in two orthogonal directions across the detector sensitive elements using the detector connector as a reference.

Figures 11 and 12 show the spatial variance of the detector for the 0.093- and 0.25-inch beam diameters, respectively. For the larger beam, the spatial response is shown to be very uniform. However, the response using the smaller beam varies by a factor of 3 due to local inhomogeneties in the detector. This deviation is not critical to the experiment since the cavity image

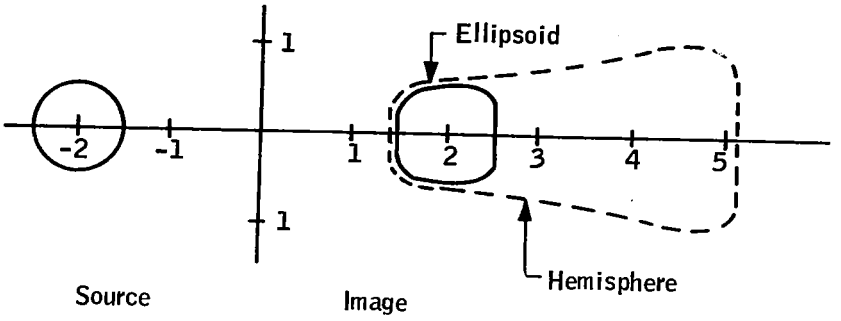

Figure 8. Relative Image Quality

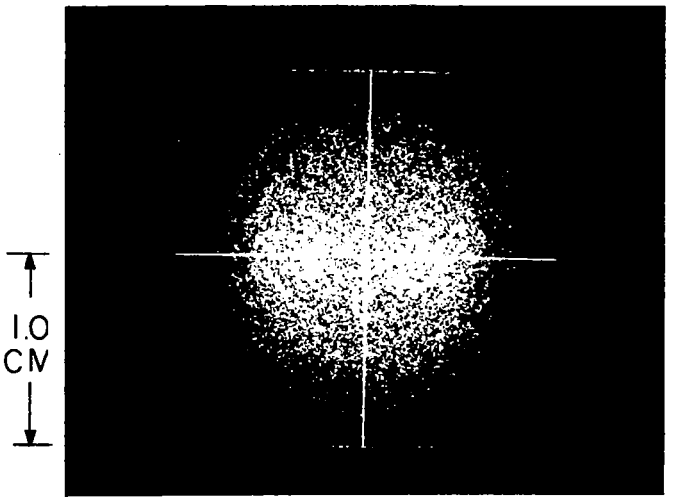

Figure 9. Theoretical Imaging of 1-cm Diameter Source

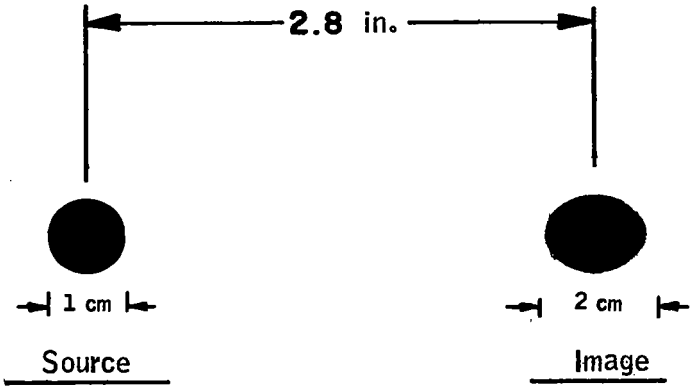

Figure 10. Experimental Determination of Ellipsoidal Reflector Quality

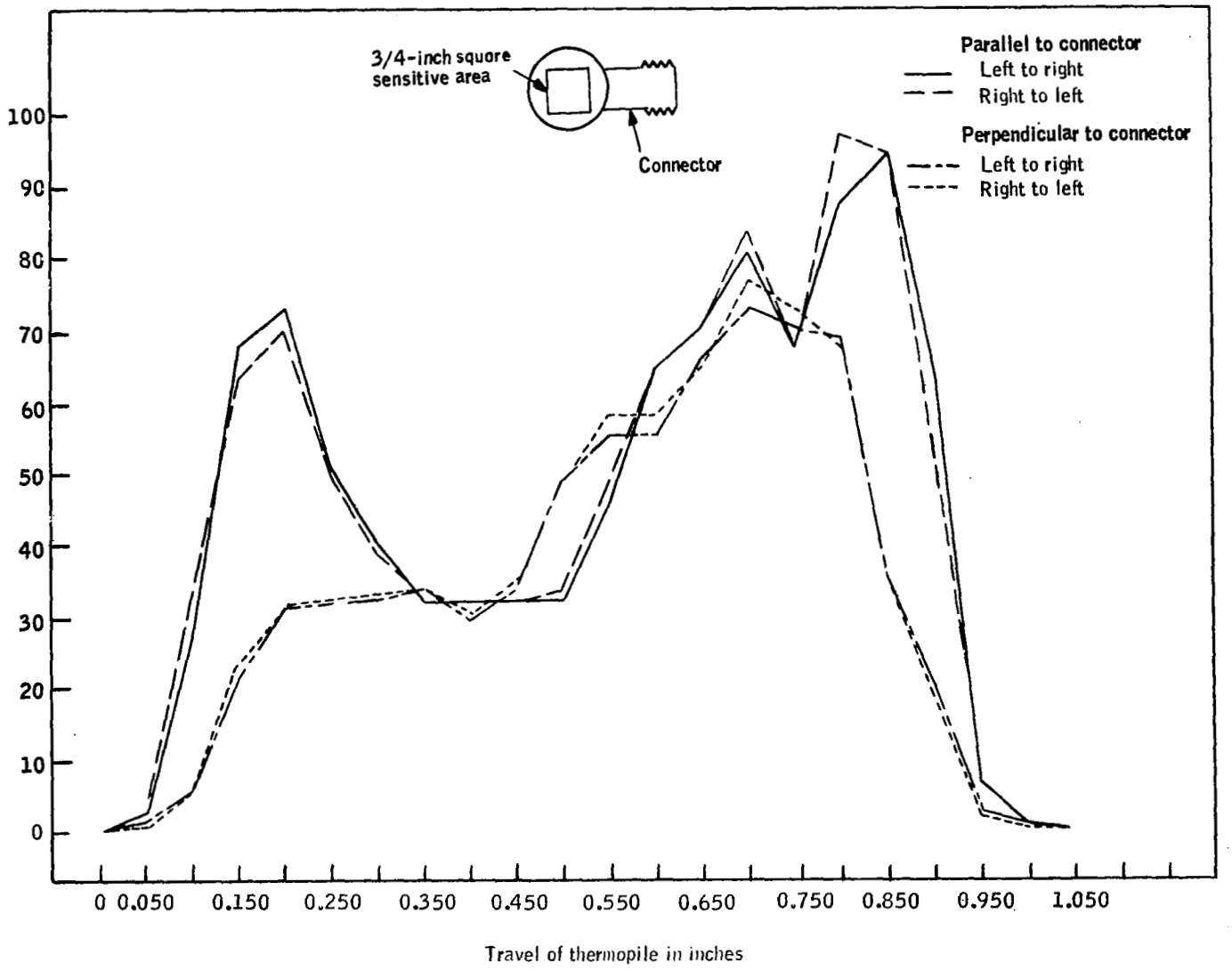

Figure 11. Spatial Sensitivity of Detector for 0.093-Inch Diameter Beam

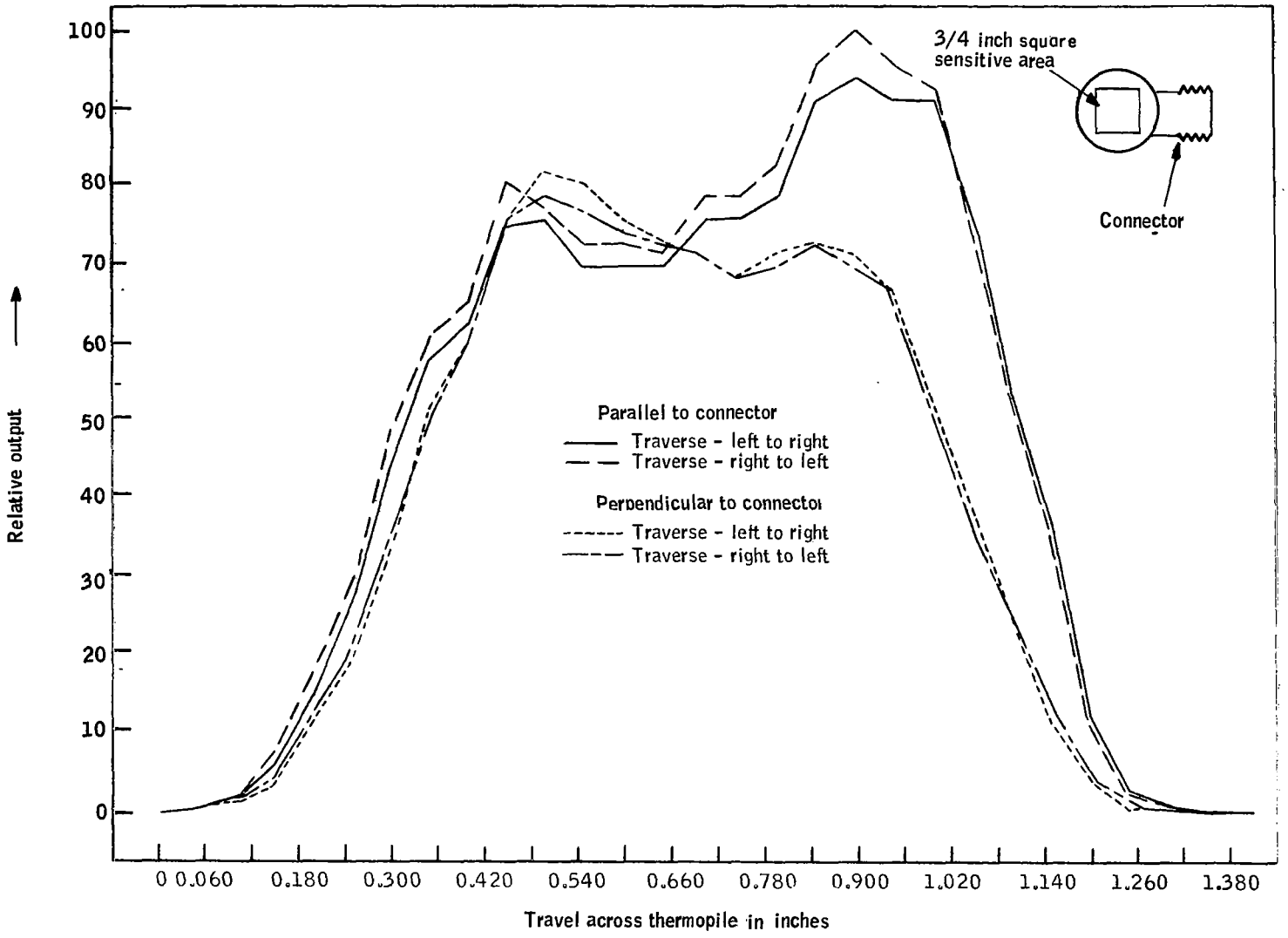

Figure 12. Spatial Sensitivity of Detector for 0.25-Inch Diameter Beam

is large and these local variations are ingegrated out. Little or no hysteresis is seen in the detector as evidenced by the similarity of the response data from right to left and left to right.

Similar measurements determined the detector angular sensitivity. Figures 13 and 14 show the measurement relative output as a function of angle of incidence for measurements made in orthogonal planes. Again, measurements were made using both the 0.093 and 0.25-inch diameter beams. The detector response shown in Figure 14 for the larger beam shows a relatively flat response out to approximately 40 degrees followed by a sharp roll-off out to 80 degrees.

Correction of the measurement data for the angular response of the detector when operating within the ellipsoidal chamber is discussed in the following error analysis section.

Error Analysis

A previous section discussed how large errors are permissible in the reflectance measurement witnout significantly affecting the determination of cavity emmitance. Table 1 lists the potential sources of error in the experiment and magnitude of the percentage error for each source.

TABLE 1. MEASUREMENT ERRORS

Detector angular response	15%
Initial calibration	3%
Ellipsoid reflectance	2%
Modulated reflections	Negligible
Atmospheric path losses	Negligible
System noise	Negligible
Laser power stability	Negligible
Cavity self emission	Negligible
Total	20%

As was previously pointed out, however, the total error of 20 percent shown in Table 1 are errors in the measurement of cavity reflectance and produce errors on the order of 0.1 to 0.01 percent in the cavity emissivity data. Each of the above errors is discussed in the following paragraphs.

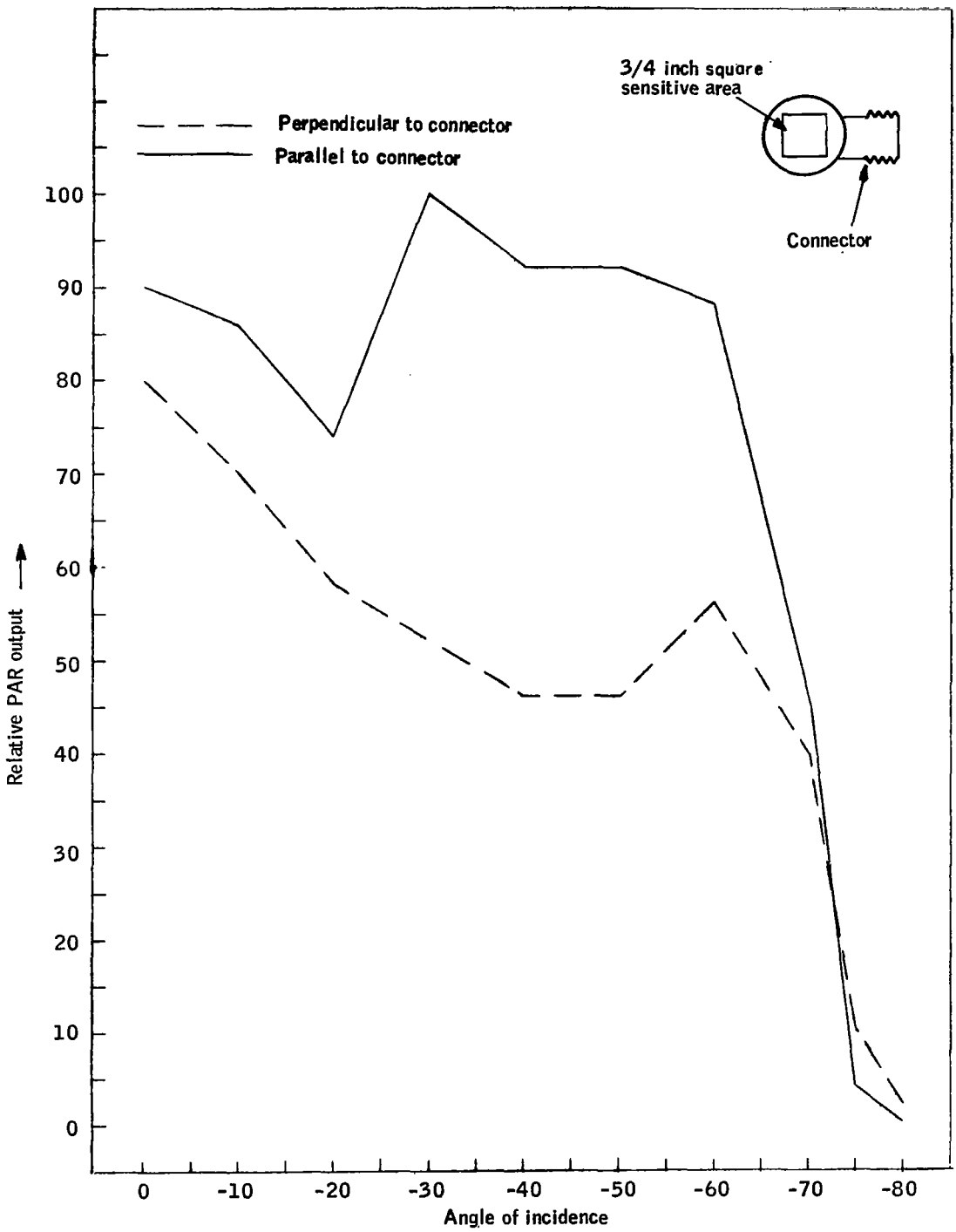

Figure 13. Angular Sensitivity of Detector for 0.093-Inch Diameter Beam

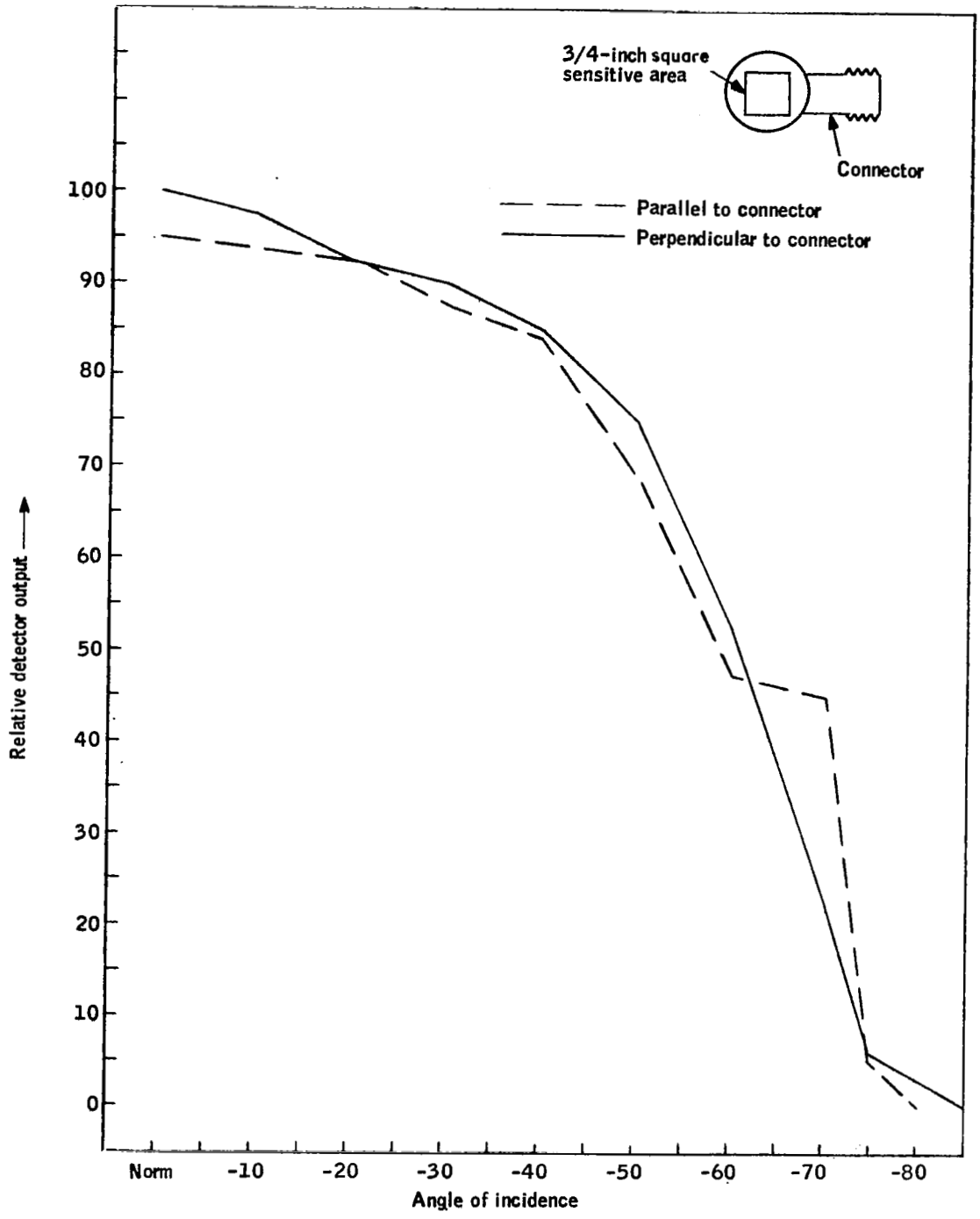

Figure 14. Angular Sensitivity of Detector for 0.025-Inch Diameter Beam

Detector angular response. -- The loss of detector sensitivity at large incidence angles is the largest potential source of error. Using the detector angular sensitivity measurements shown in Figure 14 and assuming the cavity aperture is imaged on the detector with a perfectly diffuse distribution (equal intensity in all directions), approximately 30 percent of the reflected energy is not detected.

In the actual experiment, however, the laser beam was incident on the cavity aperture at angles from the normal up to 30 degrees. Therefore, the directional hemispherical emittance would be skewed toward the normal which would reduce the field of view error. This error magnitude would then be dependent on the laser beam incidence angle.

In the system calibration, the energy loss due to the detector angular response was taken into account. However, due to the uncertainty of the actual directional hemispherical reflectance characteristics, the error caused by detector angular response was estimated to be a maximum of 15 percent.

Initial calibration. -- Calibration of the detector-electronics was accomplished using standard calcium flouride attenuators and a stable laser source. Vendor data stated a 0.093 transmission factor, and the tests conducted of each individual attenuator and the attenuators in multiple series verified the vendor data.

Repeatability of the initial calibration readings was approximately three percent; this error being caused by misalignment due to the insertion and extraction of individual attenuator elements.

Ellipsoid reflectance. -- Reflectance values for the ellipsoidal surface were determined from reflectance measurements of varying quality substrate samples coated at the same time as the ellipsoid. Appendix C details the tests and results that were conducted. Reflectance values for the samples varied from 0.87 for poor quality substrate to 0.94 for high quality substrate.

Inspection of the ellipsoidal surface indicated a high quality surface and, therefore, a reflectance value of 0.93 was used. As indicated in Table 1, an allowable error of 2 percent was estimated for this reflectance value and it was not significant in affecting the experiment data. Further analysis conducted during calibration of the measurement system substantiated the 0.93 reflectance value.

Modulated reflections. -- If the laser beam is larger than one centimeter as the beam enters the cavity aperture, modulated energy will be reflected off the cavity shoulder and be focused onto the detector. Measurement of the laser beam characteristics, discussed in a previous section, indicated that the laser energy incident on the cavity shoulder would be approximately five orders of magnitude below the main beam peak.

For measurement of this modulated energy reflection, a dummy cavity was placed in the experiment that permitted all energy entering a one-centimeter aperture to be absorbed external to the test setup (see Figure 4). Measurement with this experiment showed that less than 10^{-7} of the incident energy

was reflected off the cavity shoulder and collected by the detector. This energy level is on the order of the detector and electronics noise so that accurate determination was not possible; however, energy levels even two orders of magnitude higher would not produce a significant error.

These measurements were conducted with a smooth metal face on the cavity. To eliminate this error from the experiment, black flock paper was placed on all cavity faces surrounding the apertures. Measurements with the paper in place resulted in an undetectable signal and, therefore, this error source is negligible.

Atmospheric path losses. -- At the working distances involved in this experiment, atmospheric path losses are insignificant. Atmospheric transmission as a function of wavelength for 1.0 to 14.0 μ indicates a transmission exceeding 70 percent per sea mile.

System noise -- The noise equivalent power was measured for the system and found to be approximately 10^{-8} watt. Actual reflectance measurements were made down to a power level of 10^{-6} watt indicating a 100:1 signal to noise level. Any system error at this signal noise level is negligible.

Laser power stability. -- Measured stability of the laser source during long measurement times was approximately 0.1 percent. Frequent measurements of the laser output power were made and measurement data corrected for this calibration.

Cavity self-emission. -- Self-emission from the cavity can cause an error if it is ac and inphase with the laser beam modulation. The absorption of the laser energy by the paint surface represent a potential source of inphase a-c heating. In addition, reflectance measurements as low as 10^{-5} are to be measured so very small a-c heating effect could possibly cause measurable signals. Consequently, a rather detailed mathematical analysis of this error source was performed.

From the analysis, presented in Appendix A, self-emission is analytically predicted to be of the order of 10^{-5}. This error is only important for the very black cavities where reflectance is of the order 10^{-5} or less. Also, such an error would tend to make the reflectance higher and emittance lower. Therefore, this error is conservative; that is, emittance values are actually blacker, so for the data presented in this report this error is negligible.

Calibration

Two techniques were used to calibrate the measurement system: The direct calibration of the detector and electronics discussed earlier, and a system measurement to check the entire experimental setup. Figure 15 presents the calibration curve determined from the results of both calibration measurements.

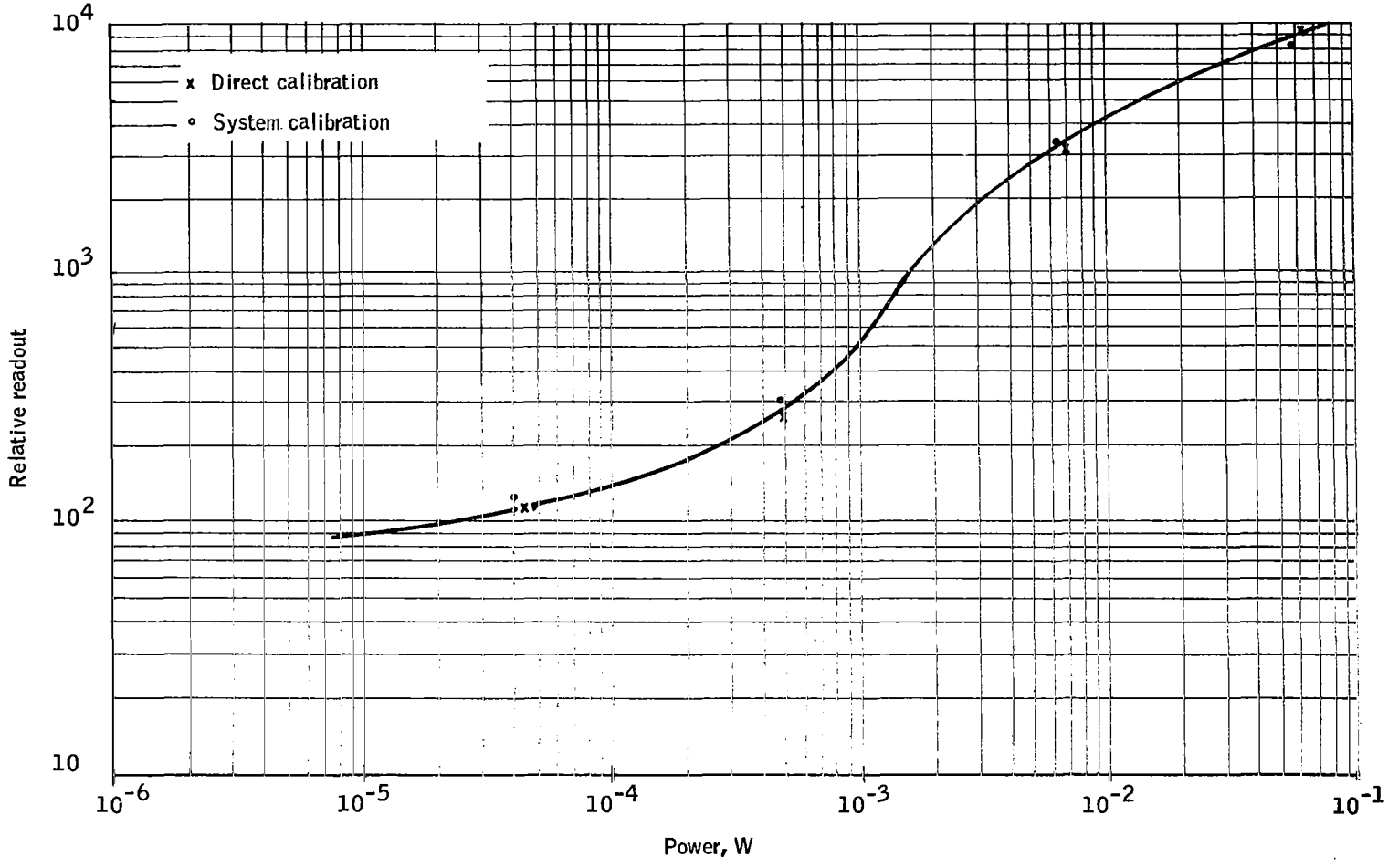

Figure 15. Calibration Curve

The system measurement was made to permit determination of the effects of detector angular response and ellipsoidal mirror reflectance on the measurement data. To make this measurement, the blackbody cavity was replaced by a copper disc painted with the black diffuse paints used to coat the cavities. Reflectometer measurements of this paint surface at 10.6 μ showed a 0.03 reflectance value.

Measurements were made using the painted disc and corrections made to the data using the sample disc reflectance, ellipsoidal mirror reflectance, and detector angular response data. Using the 0.93 reflectance data for the ellipsoid and an 85 percent correction for the detector angular response, these experimental data are compared with the direct calibration data on Figure 15. Using this data, each of the reflectance measurements taken were corrected for the mirror reflectance and the detector angular response effects.

System alignment was accomplished using the straight through cavity used in the reflected modulation experiment. The laser was aligned to the cavity entrance aperture when the output electronics indicated an undetectable output signal. Subsequent alignment of the individual blackbody cavities was assured by the test fixture.

EXPERIMENTAL RESULTS

Each individual cavity was mounted in the test fixture with the laser energy input normal to the cavity aperture. Measurements were made at five degree increments out to a maximum of thirty degrees from the normal. For the right circular cylindrical and conical cavities, the above incidence angle measurements were conducted without reference to the azimuth of the symmetrical cavities. However, for both the off-axis conical cavities, directional emittance is dependent on the angular orientation.

For a convenient reference, zero degree reference was defined as that reference when the apex of the conical cavities was toward the laser. Measurements were taken at 0, 90, 180, and 270 degrees in this reference system.

Each of the cavities were tested with both nominally specular and nominally diffuse paint coatings. Additionally, the 12.45 L/D, off-axis cone was tested with no paint coating. This was done to determine the effect of varying surface emissivities within the cavity, the emissivity of the paints being in excess of 0.90 and the emissivity of the copper surface being approximately 0.05.

The experiments conducted and results are described in the following sections, each of which is characterized by the surface conditions within the cavity interiors.

SPECULARLY REFLECTING CAVITY SURFACES

The cavity emittance results corresponding to nominally specular surfaces are summarized in Table 2 for the four configurations. The angles θ and γ, shown in Figure 16, define the spatial orientation of the directional emittance. The azimuthal angle γ is relevant only for the off-axis cones, which are not axi-symmetric.

An overall inspection of the table indicates that the emittance of the off-axis cones exceeds those of the cylindrical and conical cavities. In particular, the 12.45 L/D cone was found to have an emittance greater than 0.99999 for all of the directions investigated. The measured emittance values for the cylindrical and conical cavities are sufficiently high to qualify these configurations for application in conventional engineering practice.

Both of the axi-symmetric cavities have directional emittances which increse as the angle θ increases, with the trend being more strongly manifested for the cylinder. The relatively lower values of ϵ for the cylinder at small θ are consistent with the relatively higher directional reflectances which should occur in this geometry at normal and near normal incidence.

The directional emittances for the off-axis cones at azimuthal angles γ of 90 degrees and 270 degrees should be identical at any given θ, provided that

TABLE 2. - DIRECTIONAL SPECTRAL (10.6μ) EMITTANCE OF CAVITIES COATED WITH A SPECULARLY REFLECTING PAINT HAVING EMITTANCE OF 0.95

θ	0°	5°	10°	15°	20°	25°	30°
Cylinder	0.960	0.985	0.9965	0.997	0.998	0.999	0.9991
Cone	0.993	0.994	0.9965	0.999	0.9993	0.9997	0.9998
Off-axis cone L/D = 3, γ = 0°	0.9987	0.9985	0.9981	0.9997	0.9982	0.9985	0.9994
Off-axis cone L/D = 3, γ = 90°	0.9993	0.9991	0.9990	0.9989	0.9991	0.9992	0.9995
Off-axis cone L/D = 3, γ = 180°	0.9990	0.9990	0.9989	0.9989	0.9990	0.9991	0.9989
Off-axis cone L/D = 3, γ = 270°	0.9994	0.9992	0.9992	0.9991	0.9992	0.9994	0.9996
Off-axis cone, L/D = 12.45	$\varepsilon > 0.99999$ for $0 \leq \theta \leq 30°$, γ = 0°, 90°, 180°, 270°						

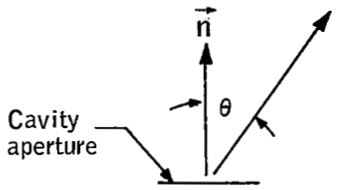

(a) Schematic elevation view

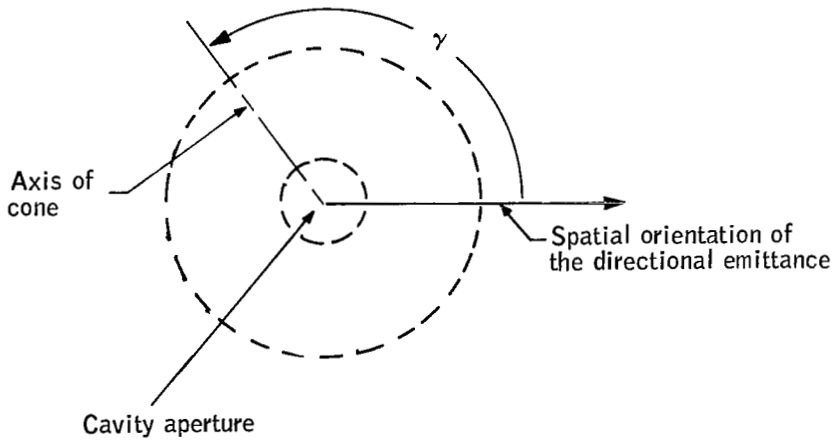

(b) Schematic plan view

Figure 16. View of Off-Axis Cone Showing the Spatial Orientation of the Directional Emittance

there are no irregularities in geometry, surface finish, coating thickness, and cavity alignment. A comparison of values for the 3 L/D, off-axis cone at γ = 90 degrees and 270 degrees shows coincidence within the expected experimental error thereby lending support to the quality of the apparatus and to the validity of the error analysis. Furthermore, it can be reasoned that the emittances for γ = 180 degrees should exceed those for 90 degrees at each fixed θ. This behavior is verified by the measurements.

The experimental results were also compared to the available predictions of analysis. A computation, based on a ray-tracing technique, for the 12.45 L/D, off-axis cone with a specularly reflecting surface (reflectance = 0.10) gave a directional emittance of > 0.99999 for $0 \leq \theta \leq 10$ degrees. This finding is in excellent agreement with that of experiment. For the cylindrical and conical cavities, extrapolation of published information for the hemispherical emittance yields 0.999 and 0.996. These values differ somewhat from those of Table 2. The level of agreement is, however, as good as can be expected in light of the aforementioned extrapolation and in view of the fact that hemispherical and directional values are being compared.

DIFFUSELY REFLECTING CAVITY SURFACES

Table 3 gives a listing of the experimentally determined directional emittances for nominally diffusely reflecting cavity surfaces. The structure of the table is identical to that of Table 2 and the angles θ and γ are defined in Figure 16 as before.

Table 3 shows that the directional emittances for the cylinder, cone, and 3 L/D off-axis cone are of similar magnitudes, ranging between 0.991 and 0.999. Furthermore, there are no evident trends in the data as a function of the angles θ and γ. This uniformity of the results is believed due to the diffuse character of the cavity surfaces and to the common L/D of these cavities.

The 12.45 L/D, off-axis cone has a slightly higher emittance than the aforementioned cavities. In the case of the 3 L/D off-axis cone, the expected coincidence (within the estimated error) of the emittance values for γ = 90 degrees and 270 degrees is once again verified by the data.

With respect to the analytical predictions, a simplified DeVos calculation for a diffusely reflecting (reflectance = 0.10) 12.45 L/D, off-axis cone yielded an apparent directional emittance of 0.9995 for $0 \leq \theta \leq 10$ degrees. The difference between this calculated emittance and the value $\varepsilon > 0.99999$ of experiment is attributed, at least in part, to the fact that the surface reflectance of the analysis was 0.1 and that of the experiment was 0.025. Analytical predictions for the cylinder and the cone are available only for the hemispherical emittance. Extrapolation of the published information to the case of cavities with surface emissivities of 0.975 yields 0.996 and 0.988 for the cylinder and the cone, respectively. The deviations of these predictions from the experimental findings may be ascribed to the same causes as were discussed in a similar comparison for Table 2.

TABLE 3. - DIRECTIONAL SPECTRAL (10.6μ) EMITTANCE OF CAVITIES COATED WITH A DIFFUSELY REFLECTING PAINT HAVING EMITTANCE OF 0.975

θ	0°	5°	10°	15°	20°	25°	30°
Cylinder	0.9965	0.9975	0.997	0.998	0.998	0.9985	0.9985
Cone	0.9950	0.9970	0.9975	0.9970	0.9900	0.9925	0.9935
Off-axis cone L/D = 3, γ = 0°	0.9935	0.9900	0.9895	0.9935	0.9935	0.9940	0.9940
Off-axis cone L/D = 3, γ = 90°	0.9965	0.9970	0.9975	0.9980	0.9990	0.9975	0.9970
Off-axis cone L/D = 3, γ = 180°	0.9925	0.9930	0.9930	0.9915	0.9965	0.9970	0.9970
Off-axis cone L/D = 3, γ = 270°	0.9965	0.9975	0.9980	0.9985	0.9990	0.9975	0.9970
Off-axis cone L/D = 12.45	$\varepsilon > 0.99999$ for $0 \leq \theta \leq 30°$, γ = 0°, 90°, 180°, 270°						

UNCOATED 12.45 L/D, OFF-AXIS CAVITY

Measurements on the uncoated 12.45 L/D off-axis cone explored the role of cavity geometry, unaided by coatings, in augmenting the emittance. The polished copper surfaces which make up the interior of the cavity have an emittance on the order of 0.05.

The measured cavity emittances are listed in Table 4 for parametric values of the angles θ and γ which have already been defined in connection with Tables 2 and 3. The dominant characteristic of the results of Table 4 is the remarkably high values attained by the cavity emittance, especially in view of the fact that the actual emittance of the cavity surfaces is very low. These high values of cavity emittance indicate that the geometry contributes enormously to the degree of blackness. Thus, it is demonstrated that high cavity emittances can be realized without coatings; the finding may have practical relevance for high temperature applications where coatings may not be stable.

All data reported herein were repeated with an interval of at least one day between the two measurements. The reflectances were repeatable to within 14.5 percent which results in repeatability on the emittance of 0.6 percent for the lowest emitting cavity and 0.0002 percent for the highest emitting cavity studied.

TABLE 4. - DIRECTIONAL SPECTRAL (10.6μ) EMITTANCE OF 12.45 L/D OFF-AXIS CONICAL CAVITY WITH A POLISHED COPPER SURFACE

θ		0°	5°	10°	15°	20°	25°	30°
γ	0°	0.935	0.965	0.885	0.935	0.895	0.985	0.960
	90°	0.940	0.935	0.950	0.955	0.940	0.945	0.950
	180°	0.940	0.940	0.970	0.900	0.920	0.85	0.895
	270°	0.940	0.940	0.945	0.950	0.955	0.945	0.955

CONCLUSIONS

A measurement technique for determining the directional spectral emittance of blackbody cavities was developed and applied to four specific cavity geometries. Error analyses, which were verified during the course of the experiments, proved the new technique to be capable of providing highly precise values of emittance. The experiment demonstrated that five significant figures could be resolved in the emittance of high emittance cavities.

One of the cavities investigated, a 12.45 L/D off-axis cone, had an emittance greater than 0.99999 when coated with nominally specularly reflecting or nominally diffusely reflecting black paints. These paints had emittance of 0.95 and 0.975, respectively. In the case in which the cavity surface were uncoated (surface emittance of approximately 0.05), measured emittances were approximately 0.95, demonstrating the effectiveness of cavity geometry in producing a high cavity emissivity.

Three other cavities having L/D = 3 were also investigated. The internal surfaces of these cavities were coated with the aforementioned black paints. The emittances of these cavities varied as low as 0.94 for the cylinder coated with specularly reflecting black paint to as high as 0.999 for all three cavities at 30° off normal.

APPENDIX A
ANALYSIS OF CAVITY FLUCTUATING SELF-EMISSION

APPENDIX A

ANALYSIS OF CAVITY FLUCTUATING SELF-EMISSION

The fluctuating self-emission from the cavity was thought to be a significant factor in contributing to the error. Initially, an analysis was made assuming the cavity wall to be semi-infinite in extent with an infinitely thin black coating on the surface of a low-conductivity material. Duhamel's integral was used to obtain solutions for a sinusoidally varying heat flux as a boundary condition. The temperature levels calculated indicated that cavity self emission was a problem. Because of those results, a more sophisticated numerical study was made of the problem to accurately determine the error.

The mathematical model used for the more detailed study is described below. The cavity was approximated by a two dimensional surface as shown in Figure A1. The surface was divided into 27 nodes for numberical purposes. The copper was assumed to be 0.25-in. thick with a 0.005-in. coating of black paint on the surface.

Mathematically, the energy transfer is described by the parabolic diffusion equation in two dimensions

$$\frac{\partial T}{\partial t} = \alpha \frac{\partial^2 T}{\partial x^2} + \frac{\partial^2 T}{\partial y^2} \tag{A1}$$

where the thermophysical properties are assumed not to be functions of temperature for simplicity.

For a time varying laser heating of one surface, the boundary condition is

$$y > |\Delta| \quad x = 0, \quad t > 0, \quad -k \frac{\partial T}{\partial x}\bigg|_{x=0} = h (T - T_\infty) + \sigma (T^4 - T_\infty^4) \tag{A2}$$

where T is the ambient temperature and the paint is assumed black (i.e., $\epsilon = 1.0$).

Finally, the second surface of the cavity convects energy away and we have

$$x = L, \text{ all } y, \quad -k \frac{\partial T}{\partial x}\bigg|_{x=L} = h (T - T_\infty) \tag{A3}$$

The heat transfer coefficient in Equation (A2) and (A3) is assumed to be representative of free convection in air (ambient temperature was assumed to be 70°F).

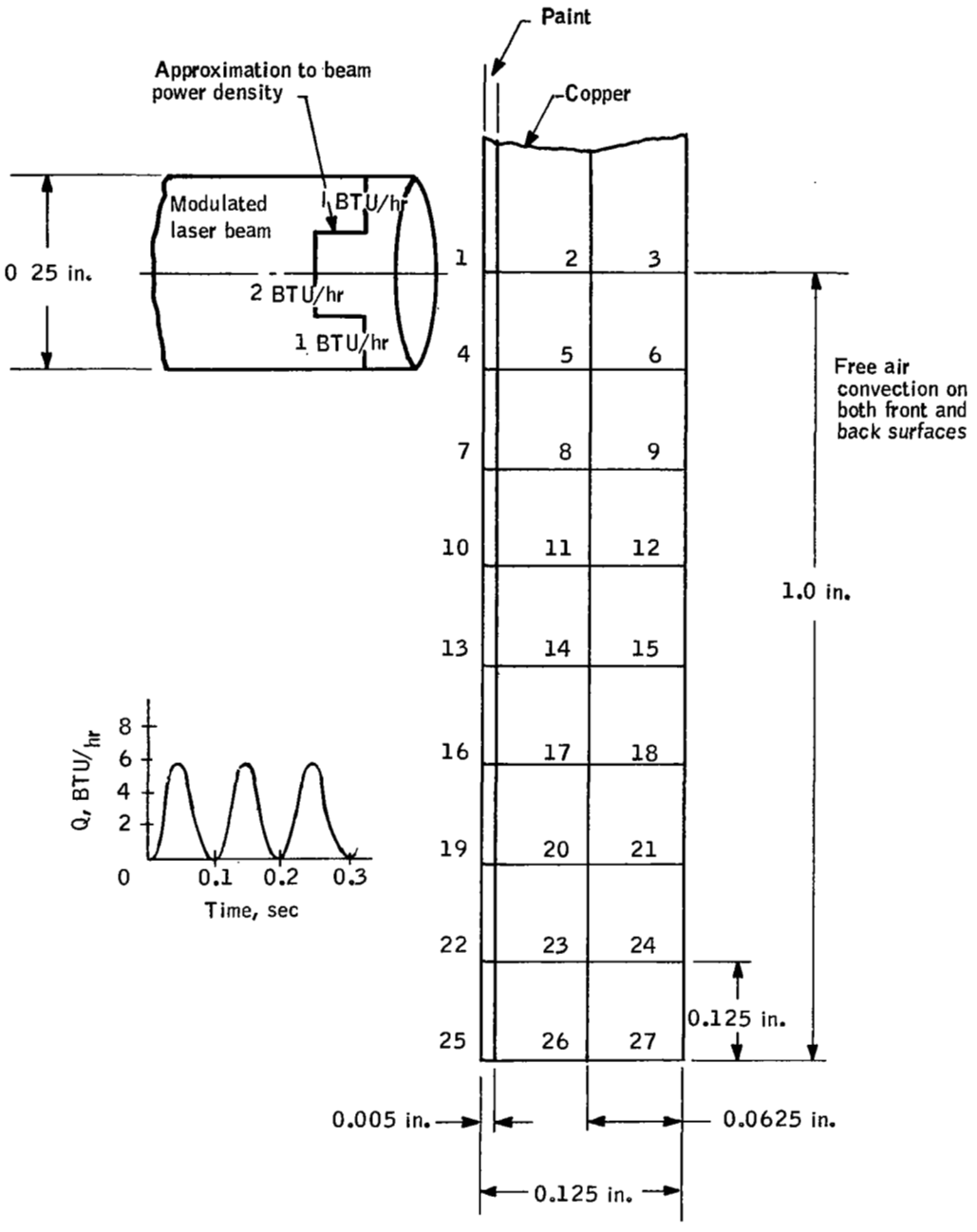

Figure A1. Geometry of Thermal Analysis

The initial conditions are

$$t = 0 \quad \text{all } x, \quad \text{all } y \quad T = T_{\infty} \tag{A4}$$

Using a standard finite difference heat conduction numerical routine (TB HEAT), Equation (A1) with associated boundary and initial conditions was solved.

The results are shown in Figure A2 for heating at nodes 1, 4, 7, and 10 of Figure A1. It is evident that, for 2 watts input, cavity heating is no problem.

The differences between this analysis and the original closed-form-problem formulated earlier are obvious. Originally, a semi-infinite slab of material was postulated. This was one component and for a conservative estimate the thermal conductivity was taken to be that of the paint (i.e., 0.5 BTU/hr ft. °F). In the latter numerical study, the paint comprised only 0.0005 inch while the copper (with thermal conductivity of 220 BTU/hr ft. °F) was 1/8 thick. Apparently, the copper dominates the system to the extent that, for practical purposes, the paint could be neglected except for the absorption of the incident radiation.

The consideration of the amount of total energy radiated due to 0.1°F change in temperature is approached as follows:

We have the Stefan Boltzmann law

$$q = \varepsilon \sigma T^4$$

Differentiating this expression with respect to temperature yields

$$dq = 4\varepsilon\sigma T^3 dT$$

and rewriting the differentials as increments

$$\Delta q = 4 \varepsilon \sigma T^3 \Delta T$$

Conservatively, assume the emissivity to be unity and obtain

$$\Delta q = 4(1)(0.173)(10^{-2})\left(\frac{500}{100}\right)^3 \Delta T$$

$$\Delta T = 0.1°F$$

$$\Delta q = 0.0865 \text{ BTU / hr ft}^2$$

Assume 0.1 in.^2 = area heated (very conservative)

$$\Delta q = \frac{0.0865}{3.41} \frac{0.1}{144} = 1.76 \times 10^{-5} \text{ watts}$$

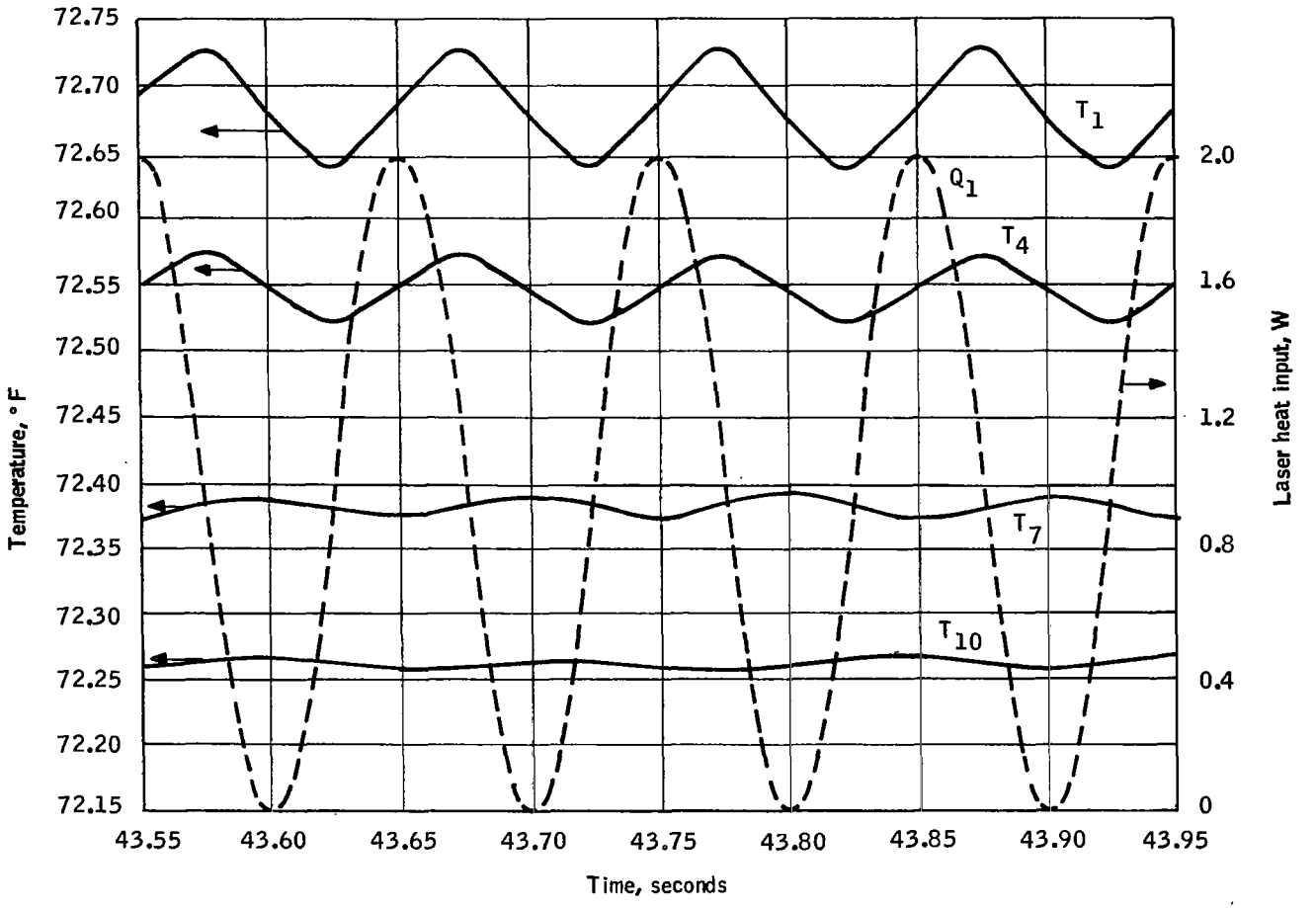

Figure A2 Cavity Heating Results

Thus, the change in total energy will be about 10^{-5} watts. However, with an incident level of 2 watts and an emissivity of 0.99999, the energy reflected to the detector is on the order of 10^{-4} watts (one order of magnitude above the calculated maximum fluctuation).

APPENDIX B
THEORY OF OPTICAL MODULATOR

APPENDIX B
THEORY OF OPTICAL MODULATOR

Modulation of the laser beam results from the variation in transmission (reflection) of the optical plates as they rotate. This is caused by the changing orientation of the plates with respect to the plane of polarization of the laser beam.

For the modulator to work, the laser beam used must be plane polarized and must maintain a fixed polarization plane. If the laser beam is completely plane polarized the degree of modulation (reflection) for a single plate is

$$M = 16\left[\frac{\sin\theta_1 \sin\theta_2 \cos\theta_1 \cos\theta_2}{\sin^2(\theta_1 - \theta_2)\cos^2(\theta_1 - \theta_2)}\right]^2 - 16\left[\frac{\sin\theta_1 \sin\theta_2 \cos\theta_1 \cos\theta_2}{\sin^2(\theta_1 + \theta_2)}\right]^2 \quad \text{(B1)}$$

The first term represents the transmission of the plate for the initial orientation shown in Figure B1 with the polarization plane parallel to the paper, and the second term represents the transmission for the plate rotated 90 deg about the laser beam as a spin axis.

To determine the effects of the second plate, the two terms in the expression are independently squared. The plot of percent modulation versus incident angle for a two-plate system is shown in Figure B1. This plot is from the expression

$$M = 256\left[\frac{\sin^2\theta_1 \cos^2\theta_1 \sin^2\theta_2 \cos^2\theta_2}{\sin^4(\theta_1 + \theta_2)\cos^4(\theta_1 - \theta_2)}\right]^2 - 256\left[\frac{\sin^2\theta_1 \cos^2\theta_1 \sin^2\theta_2 \cos^2\theta_2}{\sin^4(\theta_1 + \theta_2)}\right]^2 \quad \text{(B2)}$$

Maximum modulation (reflection) occurs at the Brewster angle for the material. The expression

$$n = \tan\theta_1$$

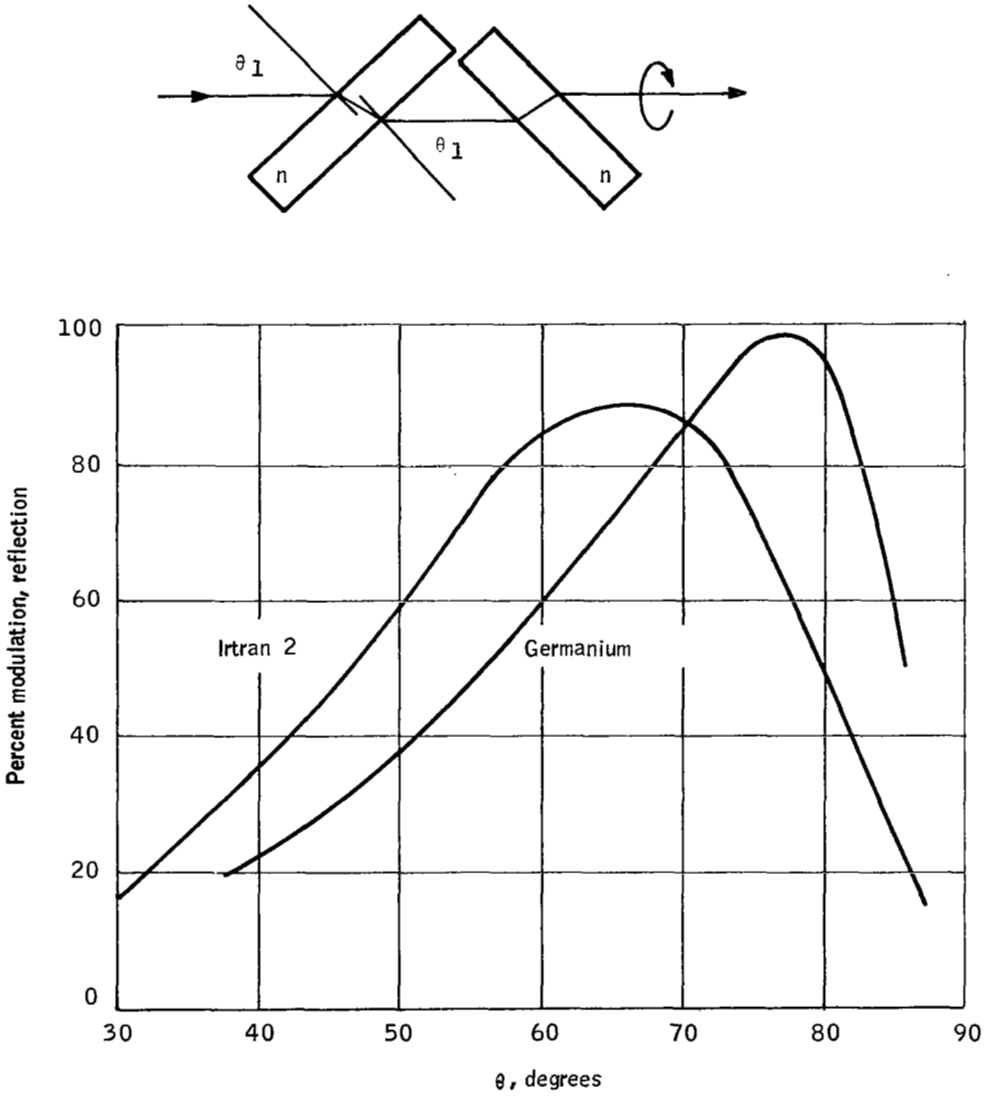

Figure B1. Modulation with Various Materials

is used to evaluate the Brewster angle where n is the index of refraction of the material. Thus, for germanium, maximum modulation occurs at about 76 deg, while for Irtran 2, maximum modulation occurs at about 67 deg. At incident angles greater than 45 deg, acceptable modulation occurs; thus, the Irtran windows were fixed at 60 deg.

APPENDIX C
INTEGRATING HEMI-ELLIPSOID

APPENDIX C
INTEGRATING HEMI-ELLIPSOID

This appendix describes the fabrication of an integrating hemi-ellipsoid used in this study and the associated analytical and experimental testing performed on it.

FABRICATION

The current hemi-ellipsoid was constructed from two quarter sections of an ellipsoid with a semi-major axis of 5.000 inches and a semi-minor axis of 4.800 inches. The distance from the center of the ellipse to each focal point is 1.4 inches.

The convex male mold was machined on a lathe by carefully adjusting the cutting tool to "x" and "y" coordinates (see Figure C1) computed on a digital computer. The "y" coordinate of the tool location was computed, accounting for the tool radius, for 0.001 increments in "x". A solid hemi-ellipsoid symmetric with respect to the semi-major axis was generated, as shown in Figure C1. The mold was highly polished to give the resulting casting a smooth finish.

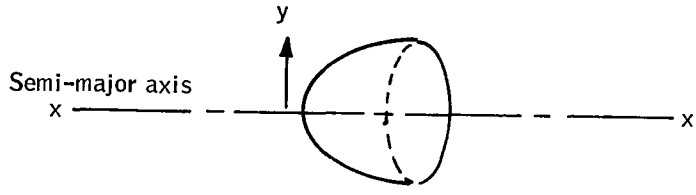

Figure C1. Convex Ellipsoid Mold

The quarter ellipsoids were prepared by filling the annulus between an aluminum outer casting and the male mold with epoxy. A very light coat of silicone vacuum grease was used as a release agent between the male mold and cast epoxy. The castings were produced with an additional one inch overlap along the mirror axis. This gave the hemi-ellipsoid an overlap as shown in Figure C2.

It was necessary to evacuate the mold while casting the epoxy to remove entrained air bubbles on the mold surface. After many tests, a complex

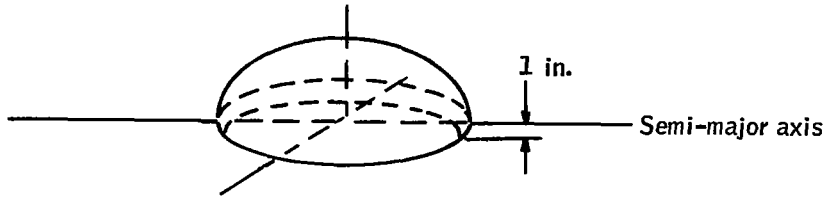

Figure C2. Hemi-Ellipsoid

pumping schedule was developed by which DEVCON F, an 80 percent aluminum filled epoxy, could be cast with a minimum of entrained bubbles.

Aluminum was evaporated on the inner surface of the ellipsoid to provide high reflectance in the spectral regions of interest. The hemi-ellipsoidal mirror appeared to have excellent focusing properties in the visible, but further evaluation was considered necessary.

THEORETICAL FOCUSING

The focusing properties of the hemi-ellipsoid were obtained using a digital computer. With vector calculus, a geometrical ray trace was performed on the hemi-ellipsoid. The hemi-ellipsoidal collector is described by Equation C1 in a rectangular cartesian coordinate system as shown in Figure C3.

$$\frac{x^2}{a^2} + \frac{y^2}{b^2} + \frac{z^2}{c^2} = 1 \qquad \text{(C1)}$$

where

$a = 5$ inches

$b = c = 4.8$ inches

Consider a ray which originates from the source point (x_1, y_1) and is reflected by the hemi-ellipsoid at an arbitrary location (x_2, y_2, z_2). The reflected ray intersects the xy-plane at the image point (x_4, y_4). The normal to the collector surface intersects the xy-plane at the point (x_3, y_3). It can be shown that

$$x_3 = 0 \qquad \text{(C2)}$$

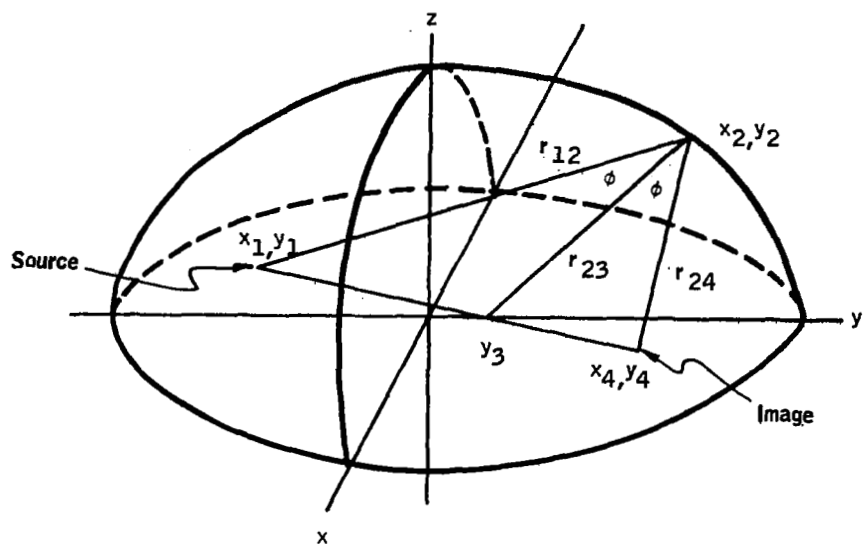

Figure C3. General Coordinate System for Ellipsoid

$$y_3 = y_2 (1 - a^2/b^2) \tag{C3}$$

Thus, the intersection of the normal with y axis is a function of where the ray strikes the surface of the ellipsoid.

Define, for convenience

$$g = a^2/b^2 \tag{C4}$$

and

$$h = \frac{r_{23}^2}{r_{12}^2 - r_{13}^2} = \frac{r_{34}}{r_{13}} \tag{C5}$$

By restricting the source and image to be in the equatorial plane of the hemi-ellipsoid (i.e., z = 0), only the ray pattern in the xy-plane need be considered. This pattern is shown in Figure C4. Using geometrical relationships, we can obtain the following expressions relating the source and the image points

$$x_4 = -x_1 h \tag{C6}$$

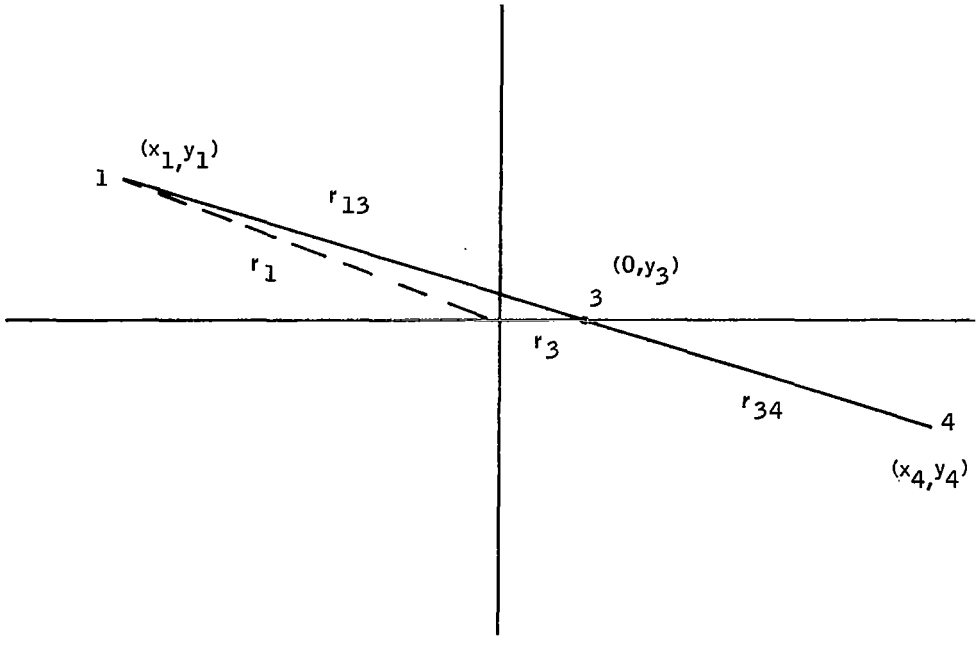

Figure C4. Two-Dimensional Coordinate System

$$y_4 = y_2 (1 - g)(1 + h) - hy \tag{C7}$$

where

$$r_{12}^2 = r_1^2 + r_2^2 - 2r_1 \cdot r_2 = x_1^2 + y_1^2 + x_2^2 + y_2^2 + z_2^2 - 2x_1x_2 - 2y_1y_2$$

$$r_{13}^2 = y_2^2 (1 - g)^2 + x_1^2 + y_1^2 - 2y_1y_2 (1 - g)$$

$$r_{12}^2 - r_{13}^2 = x_2 (x_2 - 2x_1) + z_2^2 + gy_2y_2 (2 - g) - 2y_1$$

$$r_{23}^2 = x_2^2 + z_2^2 + g^2y_2^2$$

Equations (C6) and (C7) were programmed on a digital computer. A diffuse circular source of energy 1 cm in diameter emitted energy from one focal point in the hemi-ellipsoid. The rays were emitted from either the boundary of the source or the entire source. The spot on the source and the direction of the emitted ray were chosen by use of a random number generator. Each ray so selected reflected from the ellipsoid and struck a point in the second focal plane. Each discrete points in the second focal plane was displayed on a large oscilloscope used as the output device of the digital computer. The data was recorded by taking a photograph of the oscilloscope display.

Part (a) of Figure C5 shows the image of the boundary of a 1-cm circular source computed with about 8000 rays emitted in a 45 deg cone about the normal. The grid lines shown on the photographs are 2-cm long for reference purposes. The image of an entire circular source radiating in a ten-degree vertical cone only is shown in (b) of Figure C5. About 10 000 rays were used. Finally, the entire circular pattern radiating in all directions is shown in (c) of Figure C5. Over 25 000 rays were used to generate the photograph. It is obvious that all of the energy emanating from the 1-cm circular source is contained within a 2-cm square about the center defined by the focal point. The inclusion of the lower portion of the hemi-ellipsoid introduces aberrations.

In most applications, the majority of the energy would leave normal to the source, with little energy leaving in directions near 90 deg from the normal. Therefore, aberrations as shown, are not serious.

The hemi-ellipsoid will perform better than an equivalent hemisphere, and it will improve the accuracy of the measurements.

EXPERIMENTAL TESTS

In addition to the theoretical analysis, experimental tests were used to evaluate the focusing properties of the ellipsoidal mirror. Although the mirror was developed for use at 10.6μ, tests were performed using visible light. If the mirror is acceptable using visible light, it will perform better in the infrared since the surface quality is less critical at longer wavelengths.

A fixture was made to accurately locate the focal points of the mirror; see Figure C6. A thin opal glass plate was placed in the fixture at one focus to serve as a diffuse source. A plexiglass block with two, six-volt light bulbs was placed on top of the diffuser plate for illumination. The diffuser plate and plexiglass block were masked to form a circular light source of one centimeter diameter in the focal plane. The image of that circular pattern was formed at the second focus. Visually, the image appeared to be about equal in size and shape to the source. Recording of the image was accomplished using photographic paper.

The source and image were photographed simultaneously by placing photographic paper in direct contact with the source and at the image plane. These photographs were shown in Figure 10, where a four second image exposure was used. This image is representative of the distortion (magnification) in the visible.

The reflectance of the ellipsoid mirror surface was evaluated by preparing specimens in the same manner as the ellipsoid mirror. These samples were aluminized simultaneously with the ellipsoid. The spectral reflectance of two specimens measured from one to ten microns is shown in Figure C7. One of these samples had a very smooth finish similar to the ellipsoid surface finish. The second specimen was porous with qualitative appearance much poorer than the worst section of the ellipsoid mirror. The reflectance is degraded by the poorer substrate surface finish.

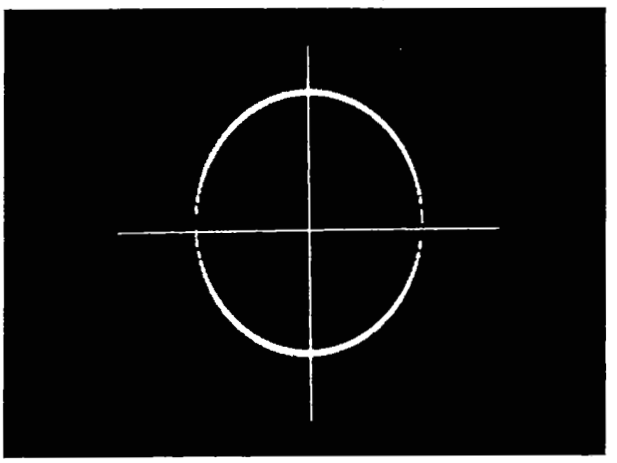

(a)

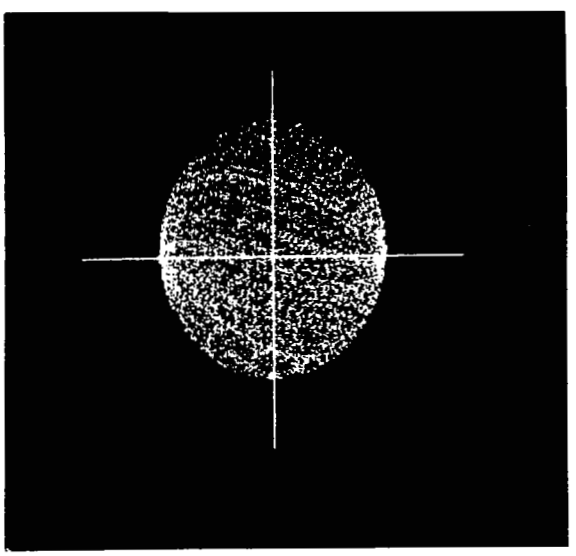

(b)

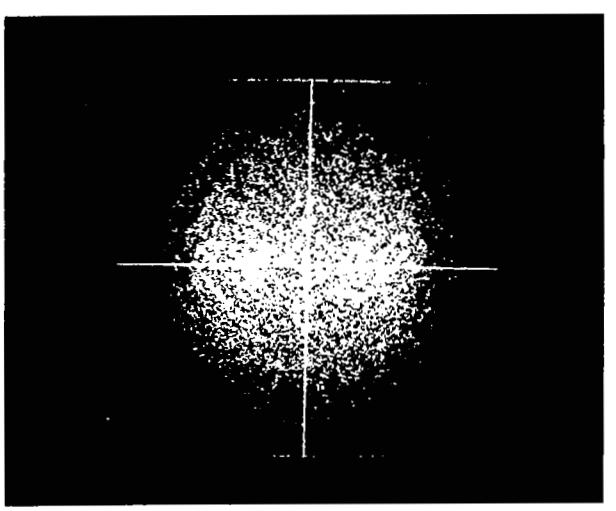

(c)

Figure C5. Analytical Determination of Ellipsoidal Reflector Image Quality

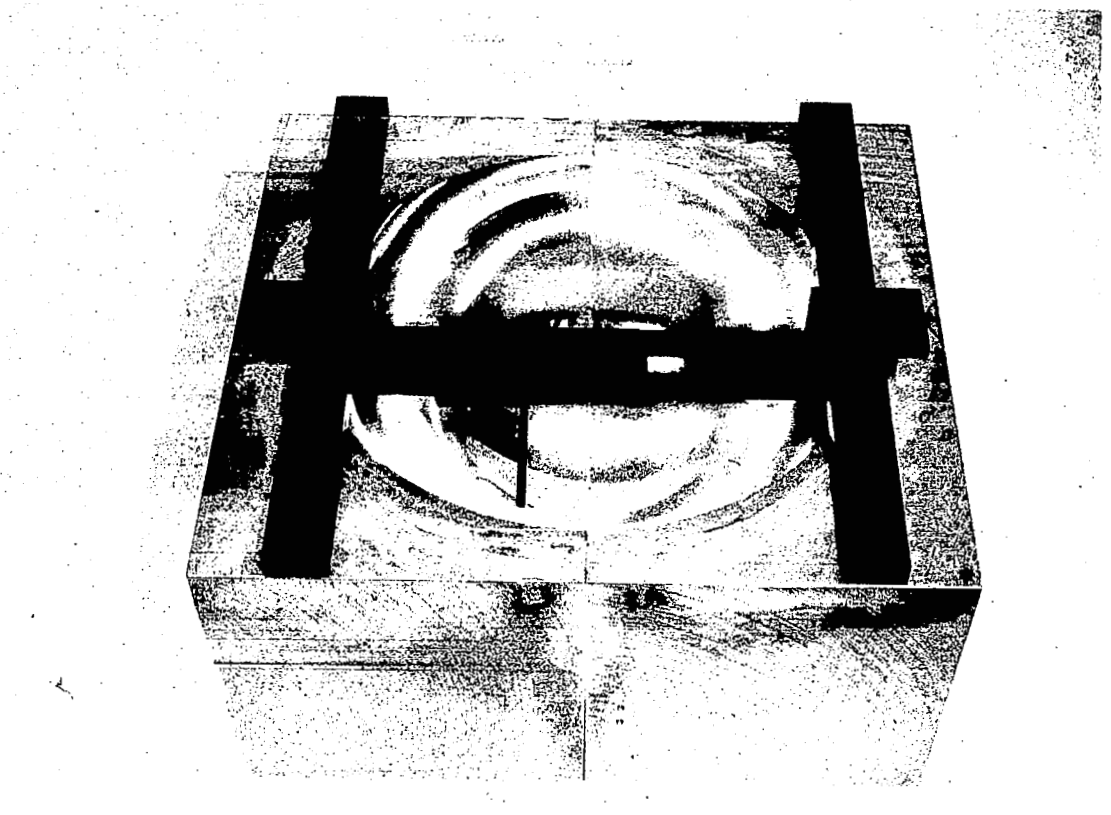

Figure C6. Focus Quality Test Fixture

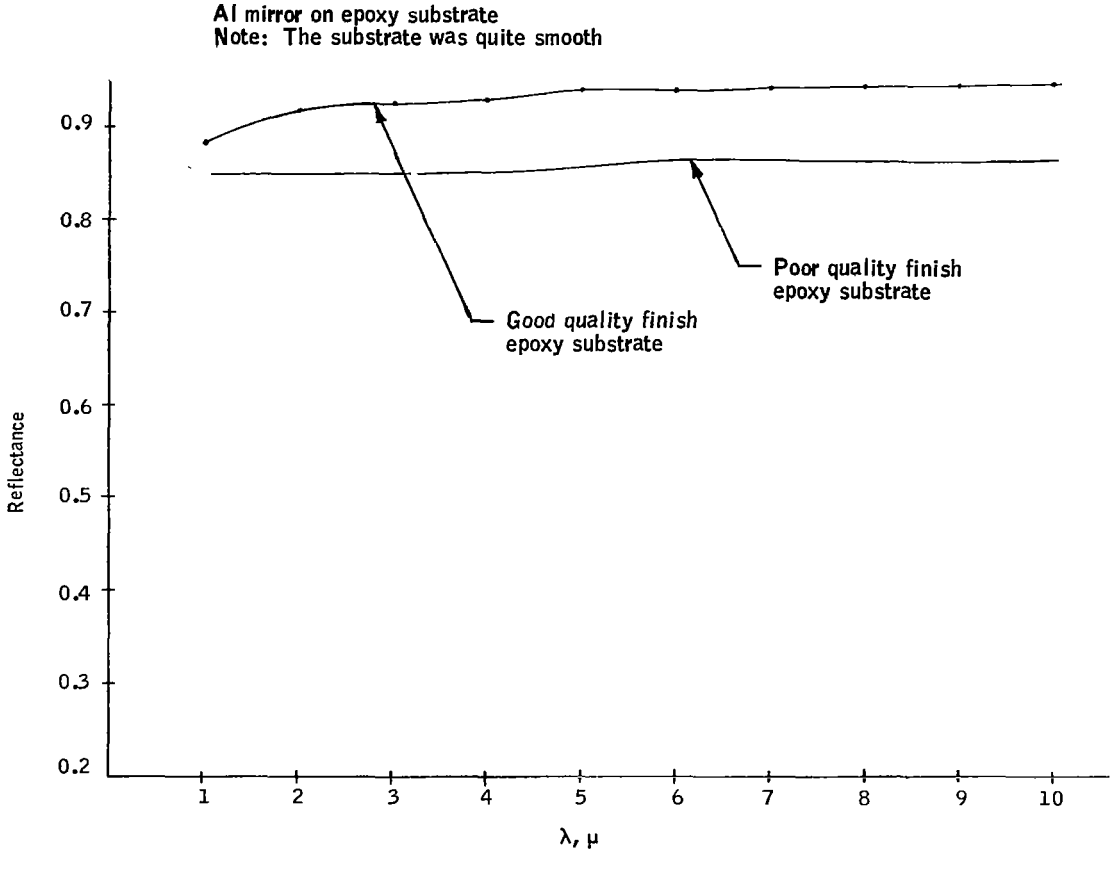

Figure C7. Reflectance of Aluminized Epoxy Specimens

BIBLIOGRAPHY

Annacker, F.; and Mannkopff, R.: Ein Reproduzier Schwarzer Strahler von 4000°K. Z. Phys., 155, p. 1, 1959.

Anon.: Blackbodies, Secondary Standards (Technical Data). Electro Optical Industries, Inc., Santa Barbara, California.

Anon.: Blackbody Radiation Sources (Technical Data). Infrared Industries, Inc., Walden, Mass.

Anselone, P.M.; and Sobel, F.: Shielding of Radiation from a Plane Circular Source. J. Opt. Soc. Am., 46, p. 934, 1956.

Beckmann, P.; and Spizzichino, A.: The Scattering of Electromagnetic Waves from Rough Surfaces. Macmillan Co., N.Y., 1963.

Bennett, H.E.; and Portius, J.O.: Relation Between Surface Roughness and Specular Reflectance at Normal Incidence. J. Opt. Soc. Am., 51, p. 123, 1961.

Birkebak, R.C.; and Cho, S.H.: Integrating Sphere Reflectometer Center - Mounted Sample Blockage Effects. ASME Paper 67-HT-54, 1967.

Birkebak, R.C.; and Eckert, E.R.G.: Effects of Roughness of Metal Surfaces on Angular Distribution of Monochromatic Reflected Radiation. Trans ASME, J. Heat Transfer, 87C, p. 85, 1965.

Black, W.Z.; and Schoenhals, R.J.: A Study of Directional Radiation Properties of Specially Prepared V-Groove Cavities. Trans. ASME, J. Heat Transfer, 90C, p. 420, 1968.

Blair, G.R.: Determination of Spectral Emissivity of Ceramic Bodies at Elevated Temperatures. J. Am. Ceramic Soc., 43, p. 197, 1960.

Brandenberg, W.M.: Focusing Properties of Hemispherical and Ellipsoidal Mirror Reflectometers. J. Opt. Soc. Am., 54, p. 1235, 1964.

Buckley, H.: On the Radiation from the Inside of a Circle Cylinder. Phil Mag, 4, p. 753, 1927, 6 p. 447, 1928, 17, p. 576, 1934.

Buzinkov, A.A., and Kozyrev, B.P.: Investigation of Atmospheric Absorption of the Radiation from a Weakly Heated Blackbody. Inz. Fiz. Zh., 9, p. 70, 1965.

Campanaro, P.; and Ricolfi, T.: Effective Emissivity of a Spherical Cavity. Appl. Optics, 5, p. 929, 1966.

Campanaro, P.; and Ricolfi, T.: New Determination of the Total Normal Emissivity of Cylindrical and Conical Cavities. J. Opt. Soc. Am., 57, p. 48, 1967.

Campanaro, P., and Ricolfi, T.: Radiant Emission Characteristics of a Non-isothermal Spherical Cavity. Appl. Optics, 5, p. 1271, 1966.

Coblentz, W.W.: The Diffuse Reflecting Power of Various Substrates. Nat. Bur. Standards Bull., 9, p. 283, 1913

Cunnold, B.A., and Milford, M.: The Blackness of a Blackbody Radiator. Phil Mag., 18, p. 561, 1934.

Davies, H.: The Reflection of Electromagnetic Waves from a Rough Surface. Proc. Inst. Elect. Engr., 101, p. 209, 1954.

Daws, L.F.: The Emissivity of a Groove. Brit. J. Appl. Phys., 5, p. 182, 1954.

DeVos, J.C.: Evaluation of the Quality of a Blackbody. Physics, 20, p. 669, 1954.

Dunkle, R.V.: Spectral Reflectance Measurements. Surface Effects on Spacecraft Material, F.J. Clauss, ed. John Wiley and Sons, Inc., p. 117, 1960.

Dunn, S.T.: Flux Averaging Devices for the Infrared. NBS Technical Note 279, 1965.

Dunn, S.T.; Richmond, J.C.; and Wiebelt, J.A.: Ellipsoidal Mirror Reflectometer. J. Research, NBS, 70C, p. 75, 1966.

Eckert, E.R.G.: Messung der Reflexion von Warmestrahlung an Technischen Oberflachen. Forsh. Gebiete Ing., 7, p. 265, 1936.

Eisenman, W.L.; and Cussen, A.J.: A Comparative Study of Several Blackbodies. Proc IRIS, 1, p. 39, 1956.

Eisenman, R.; Bates, R.L.; and Merriam, J.D.: Black Radiation Detector. J. Opt. Soc. Am., 53, p. 729, 1963.

Fecteau, M.L.: The Emissivity of a Diffuse Spherical Cavity. Appl. Optics, 7, p. 1363, 1968.

Gouffe, A.: Corrections d'ouverture des corps-noirs artificiels compte tenu des diffusions multiples internes. Rev. d'Optique, 24, p. 1, 1945.

Hardy, A.C.; and Pineo, D.W.: Errors Due to Finite Size of Holes and Sample in Integrating Spheres. J. Opti. Soc. of Am; 21, p. 502, 1931.

Hering, R.G.; and Degenhart, T.: Radiant Energy Transport Through a Circular Tube. Trans ASME, J. Heat Transfer, 90C, p. 489, 1968.

Hering, R.G.; Houchens, A.F.; and Smith, T.: Theoretical Study of Radiant Heat Exchange for Non-Gray and Non-Diffuse Surfaces in a Space Environment. Final Report NASA Research Grant No. 14-005-036, 1966.

Herold, L.M.; and Edwards, D.K.: Bidirectional Reflectance Characteristics Rough, Sintered Metal and Wire Screen Surface Systems. AIAA J., 4, p. 1802, 1966.

Hottel, H.C.; and Keller, J.D.: Effect of Reradiation on Heat Transmission in Furnaces and Through Openings. Trans. ASME, 55, p. 39, 1933.

Hurst, C.: The Emission Constants of Metals in the Near Infrared. Proc. Royal Soc. London, 142A, p. 466, 1933.

Janssen, J.E.; and Torberg, R.H.: Measurement of Spectral Reflectance Using an Integrating Hemisphere. Measurement of Thermal Radiation Properties of Solids, NASA SP-31, J.C. Richmond, ed., 1963.

Jenkins, F.A.; and White, H.E.: Fundamentals of Optics, McGraw-Hill Book Co. Inc., 1957.

Kelly, F.J.: An Equation for the Local Thermal Emissivity at the Vertex of a Diffuse Conical or V-Groove Cavity. Appl. Opt., 5, p. 925, 1967.

Kelly, F.J.; and Moore, D.G.: A Test of Analytical Expressions for the Thermal Emissivity of Shallow Cylindrical Cavities. Symposium on the Thermal Radiation of Solids, NASA SP-55, S. Katzoff, ed., p. 117, 1965; also published in Appl. Optics, 4, p. 31, 1965.

Kneissl, G.J.; Richmond, J.C.; and Wiebelt, J.A.: A Laser Source Integrating Sphere for the Measurement of Directional, Hemispherical Reflectance at High Temperatures. AIAA Paper 67-300, presented at AIAA Thermophysics Specialist Conference, New Orleans, La, April 1967.

Kostkowski, H.J.: A New Radiometric Equation and Its Application. App. Optics, 5, p. 1959, 1966.

Kozyrev, B.P.; and Buzinkov, A.A., Author's Certificate No. 164077 of 10 June 1964.

Kozyrev, B.P.; and Buzinkov, A.A.: The Design and Construction of a Blackbody. (in Russian), Izv. VUZ., Priborstroenie, 7, p. 3, 1964.

Kozyrev, B.P.; and Vershinin, O.E.: Determination of Spectral Coefficients of Diffuse Reflection of Infrared Radiation from Blackened Surfaces. Optics and Spectroscopy (in Russian), 6, p. 345, 1959.

Kruse, P.W.; McGlauchlin, L.D.; and McQuistan, R.B.: Elements of Infrared Technology, John Wiley and Sons, Inc., 1962.

LaRocca, A.; and Zissis, G.: Field Sources of Blackbody Radiation. Rev. Sci. Instr., 30, p. 200, 1961.

Leontovich, M.A.: Statistical Physics. (in Russian), Moscow, Tech. Theor. Press, 1961.

Lichtenberg, A.J.; and Sesnic, S.: Absolute Radiation Standard in the Far Infrared. J. Opt. Soc. Am., 56, p. 75, 1966.

Liebmann, G.: Ein Einfacher Schwarzer Korper. Zeis. Tech. Physik, 12, p. 433, 1931.

Lin, S.H.; and Sparrow, E.M.: Radiant Interchange Among Curved Specularly Reflecting Surfaces. Trans ASME, J. Heat Transfer, 87C, p. 299, 1965.

Maki, A., Stair, R.; and Johnston, R.G.: Apparatus for the Measurement of the Normal Spectral Emissivity in the Infrared. J. Research, NBS, 64c, p. 99, 1960.

Mendenhall, C.E.: Astrophysics J., 37, p. 380, 1915.

Munch, B.: Die Richtungsverteilung bei der Reflexion von Warmestrahlung und ihr Einfluss auf die Warmeubertragung. translated as NASA TT-F 497.

Neu, J.T.: Design, Fabrication, and Performance of an Ellipsoidal Spectro-reflectometer. NASA CR-73193, March 1968.

Nicodemus, F.E.: Emissivity of Isothermal Spherical Cavity with Gray Lamberton Walls. Appl. Optics, 7, p. 1359, 1968.

Nicodemus, F.E.: Radiance. Am. J. Phys., 31, p. 368, 1963.

Nivert, L.J.; Mulbranden, M.; and Richmond, J.C.: Primary Reference Standards of Spectral Radiance in the Infrared. Presented at the 1967 Annual Meeting JOSA, Sheratin - Cadillac Hotel, Detroit, Michigan, Oct. 10-13, 1967.

Paschen, Von F.: Uber die Verteihlung der Energie im Spectrum des Schwarzen Korpers bei niederen Temperaturen. Gesammtsitzung, 27, p. 405, 1899.

Peavy, B.A.: A Note on the Evaluation of Thermal Radiation Characteristics of Diffuse Cylindrical and Conical Cavities. J. Research, NBS, 70C, p. 139, 1966.

Perlmutter, M.; and Howell, J.R.: A Strongly Directional Emitting and Absorbing Surface. Trans. ASME, J. Heat Transfer, 85C, p. 282, 1963.

Planck, M.: The Theory of Heat Radiation. Springer-Verlag, Berlin, 1914, also Dover Pubs.

Polgar, L.G.; and Howell, J.R.: Directional Radiative Characteristics of Conical Cavities and Their Relation to Lunar Phenomena. AIAA Paper 65-669 presented at the AIAA Thermophysics Specialist Conference, Monterey, California, Sept. 13-15, 1965.

Psarouthakis, J.: Apparent Thermal Emissivity from Surfaces with Multiple V-shaped Grooves. AIAA J., 1, p. 1879, 1963.

Quinn, T.J.: The Calculation of the Emissivity of Cylindrical Cavities Giving Near Blackbody Radiation. Brit. J. Appl. Phys., 18, p. 1105, 1967.

Ribaud, G.: Traite de Pyrometric Optique, p. 231, 1931.

Richmond, J.C.; Dunn, S.T.; DeWitt, D.P.; and Hayes, W.D.: Procedures for Precise Determination of Thermal Radiation Properties - November 1963 to October 1964, NBS Technical Note 267, 1965.

Sanders, C.L.; and Stevens, B.A.: Le Pouvoir E'missif d'un Corps Noir Cylindrique. Rev. D'Optique, 33, p. 179, 1954.

Schumacher, P.E.: A High Temperature Circular Aperture Blackbody Radiation Source. Symposium on the Thermal Radiation of Solids, NASA SP-55, S. Katzoff, ed., p. 233, 1964.

Schumacher, P.E.: The Emissivity of the Rocketdyne Circular Aperture Blackbody Radiation Source. Research Rept. 63-3, Rocketdyne Div. North American Av. Inc., Canoga Park, California, 1963.

Simmons, F.; DeBell, A.G.; and Anderson, Q.S.: A 2000° C Slit-Aperture Blackbody Source. Rev. Sci. Inst., 32, p. 1265, 1961.

Smith, R.A.; Jones, F.E.; and Chasman, R.P.: The Detection and Measurement of Infrared Radiation. Oxford University Press, London, 1957.

Sparrow, E.M.: Radiant Absorption Characteristics of Concave Cylindrical Surfaces. Trans. ASME, J. Heat Transfer, 84C, p. 283, 1962.

Sparrow, E.M.: Radiant Emission, Absorption, and Transmission Characteristics of Cavities and Passages. Symposium on Thermal Radiation of Solids, NASA SP-55, S. Katzoff, ed., p. 103, 1965.

Sparrow, E.M.: Radiant Emission Characteristics of Nonisothermal Cylindrical Cavities. Appl. Optics, 4, p. 41, 1965.

Sparrow, E.M.; Albers, L.V.; and Eckert, E.R.G.: Thermal Radiation Characteristics of Cylindrical Enclosures. Trans. ASME, J. Heat Transfer, 84C, p. 73, 1962.

Sparrow, E.M.; and Cess, R.D.: Radiation Heat Transfer. Brooks/Cole Publishing Co., Belmont, California, 1966.

Sparrow, E.M.; and Gregg, J.L.: Radiant Emission from a Parallel-Walled Groove. Trans. ASME, J. Heat Transfer, 84C, p. 270, 1962.

Sparrow, E.M.; and Jonsson, V.K.: Absorption and Emission Characteristics of Diffuse Spherical Enclosures. Trans. ASME, J. Heat Transfer, 84C, p. 188, 1962.

Sparrow, E.M.; and Jonsson, V.K.: Radiant Emission Characteristics of Diffuse Conical Cavities. J. Opt. Soc. Am., 53, p. 816, 1963.

Sparrow, E.M.; and Lin, S.H.: Absorption Characteristics of a Specularly Reflecting Cylindrical Cavity Irradiated by an Obliquely Inclined Ray Bundle. Appl. Optics, 4, p. 277, 1965.

Stair, R.; Johnston, R.G.; and Halbach, E.W.: Standard of Spectral Radiance for the Region of 0.25 to 2.6 Microns. J. Research, NBS, 64A, p. 291, 1960.

Streed, E.R.; McKellar, L.D.; Rolling, R; and Smith, C.A.: Errors Associated with Hohlraum Radiation Characteristics Determinations. NASA SP-31, J.C. Richmond ed., p. 237, 1963.

Taylor, J.H.; Rupert, C.S.; and Strong, J.: The Use of a Tungsten Glower as a Source for Infrared Spectroscopy. J. Opt. Soc. Am., 41, p. 289, 1951.

Titus, J.S.; and Schmidt, R.N.: Feasibility Investigation of a Low Temperature, Variable Infrared Source. NASA CR 66614, 1968.

Torrance, K.E.; and Sparrow, E.M.: Biangular Reflectance of an Electric Nonconductor as a Function of Wavelength and Surface Roughness. Trans. ASME, J. Heat Transfer, 87C, p. 283, 1965.

Torrance, K.E.; and Sparrow, E.M.: Theory for Off-Specular Reflection from Roughened Surfaces. J. Opt. Soc. Am., 57, p. 1105, 1967.

Treat, C.G.; and Wilden, M.W.: Investigation of a Model for Bidirectional Reflectance of Rough Surfaces. AIAA Paper No. 69-64, presented at the AIAA 7th Aerospace Sciences Meeting, Jan 20-22, 1969.

Torrance, K.E.; and Sparrow, E.M.: Off Specular Peaks in the Directional Distribution of Reflected Thermal Radiation. Trans ASME, J. Heat Transfer, 88C, p. 223, 1966.

Truenfels, E.W.: Emissivity of Isothermal Cavities. J. Opt. Soc. Am., 53, p. 1162, 1963.

Usiskin, C.M.; and Siegel, R.: Thermal Radiation from a Cylindrical Enclosure with Specified Wall Heat Flux. Trans. ASME, J. Heat Transfer, 82C, p. 369, 1960.

Vollmer, J.: Study of the Effective Thermal Emittance of Cylindrical Cavities. J. Opt. Soc. Am., 47, p. 926, 1957.

Whitney, L.V.: The Temperature Scales of Columbium, Thorium, Rhodium, and Molybdenum at 0.667μ. Phys. Rev., 48, p. 458, 1935.

Wien, W.; and Lummer, O.: Wid. Ann. Phys., 56, p. 451, 1895.

Williams, C.S.: Discussion of the Theories of Cavity Type Sources of Radiant Energy. Appl. Optics, 51, p. 564, 1961.

Wolfe, W.L., ed.: Handbook of Military Infrared Technology. ONR, Wash., D.C., 1965.

Yamada, H. Y.: A High-Temperature Blackbody Radiation Source. Appl. Optics, 6, p. 357, 1967.

Yamauti, T.: Recherche-d'un Radiateur Integral au moyen d'un Corps Cylindrique. Commission Int. des P. et M. Proc. Verb., 16, p. 243, 1933.

Zhulev, Yu. G.: Emissive and Absorptive Power of Trapezoidal Grooves. Teplofizika Vysokikh Temperature (in Russian), 5, p. 480, 1967.

Zipin, R. B.: The Apparent Thermal Radiation Properties of an Isothermal V-Groove with Specularly Reflecting Walls. J. Research, NBS, 70C, p. 275, 1966.

NASA-Langley, 1970 —— 23 CR-1583